2016•2017
FACULTEIT GENEESKUNDE EN LEVENSWETENSCHAPPEN
master in de biomedische wetenschappen

Masterproef

Dental pulp stem cell therapy in ischaemic stroke: exploring the neuroprotective and -regenerative effects *in vitro*

Promotor :
Prof. dr. Annelies BRONCKAERS

Copromotor :
dr. Esther WOLFS

Hannelore Kemps

Scriptie ingediend tot het behalen van de graad van master in de biomedische wetenschappen

2016•2017
FACULTEIT GENEESKUNDE EN LEVENSWETENSCHAPPEN
master in de biomedische wetenschappen

Masterproef

Dental pulp stem cell therapy in ischaemic stroke: exploring the neuroprotective and -regenerative effects *in vitro*

Promotor :
Prof. dr. Annelies BRONCKAERS

Copromotor :
dr. Esther WOLFS

Hannelore Kemps

Scriptie ingediend tot het behalen van de graad van master in de biomedische wetenschappen

universiteit hasselt | Maastricht University

Acknowledgements

Since the start of my education as biomedical scientist, I was intrigued about the courses of neurology. After performing my bachelor training in the group of Neurophysiology, I knew from that point onwards that I would like to pursue a biomedical career in the fascinating field of neuroscience. Hence, it was a great opportunity for me to perform my senior master internship on this project in the research group of Morphology. During the last 8 months, I learned a lot of new skills as biomedical researcher and got to know many new people. Moreover, I experienced that in science, you are never fully prepared for what can happen. As a great mind once said: "Science never solves a problem without creating ten more." However, by working together as a team, every problem can be solved. Therefore, I would like to express my gratitude to several people.

First of all, I would like to thank my promotor Prof. dr. Annelies Bronckaers for her trust and guidance throughout this experience. Her joy and passion for research set a great example for many young researchers like me. I am very grateful for the opportunity that she gave me to pursue a PhD in her research group. I am certain that she will be an excellent promotor and that her criticism will help me to become a better scientist.

Furthermore, I would like to thank my co-promotor dr. Esther Wolfs for her critical view and advice on my work. Her ideas during our lab meetings have helped me as a researcher to expand my critical scientific thinking skills. In addition, she introduced me to the basics of cloning and taught me that cloning requires a lot of patience and even more luck ☺. I also would like to thank my second examiner dr. Jeroen Bogie for reviewing my project with a critical view and his suggestions during our progress meetings.

Special thanks goes to my daily supervisor Yörg Dillen for his guidance during the experimental work and his revision of my master thesis. He gave me the responsibility to plan my own experiments and to work independently in the lab. I will never forget our nice talks and his ability to remain calm under (almost) every (OGD) situation ☺. I wish you all the best with the rest of your PhD career.

A word of appreciation goes to all the members of the Morphology group for creating a pleasant working atmosphere. They were always there to help me out and answer my questions. Also, many thanks for Marc Jans and Jeanine Santermans for the help with the electron microscope and sectioning of our chondrogenic cell pellets.

Of course, a huge thanks goes to my fellow students at BIOMED. Jana, Melissa, Paulien, Lize and Yassin, I would like to thank you for the support and the crazy talks we had to keep each other sane. Thanks to you guys, 'greasy Friday' has been taken to a whole new level. I wish you all the best of luck in the future! Finally, I would like to thank my parents, grandparents, my sister and my boyfriend for the continuous support during my education and for giving me the opportunity to pursue my dreams.

Table of contents

List of abbreviations

ALP Alkaline phosphatase

AMPA α-amino-3-hydroxy-5-methyl-4-isoxazole propionic acid

BBB Blood-brain barrier

BDNF Brain-derived neurotrophic factor

bFGF Basic fibroblast growth factor

BLI Bioluminescence imaging

BM-MSC Bone marrow-derived mesenchymal stem cells

CM Conditioned medium

CXCR4 Chemokine receptor type 4

DAPI 4,6-diamidino-2-phenylindole

DMEM Dulbecco's modified Eagle's medium

DMSO Dimethyl sulfoxide

DPSC Human dental pulp stem cells

EGF Epidermal growth factor

FABP-4 Fatty acid binding protein 4

FBS Foetal bovine serum

FDA Food and Drug Administration

FI Fluorescence intensity

Fibr Fibronectin

Fluc Firefly luciferase

GDNF Glial cell-derived neurotrophic factor

GF Growth factors

HBSS Hanks balanced salt solution

HDF Human dermal fibroblasts

IGF-I Insulin-like growth factor I

IGF-II Insulin-like growth factor II

IGFBP-6 Insulin-like growth factor binding protein 6

IGF1R Insulin-like growth factor receptor type 1

IL-1β Interleukin 1 bèta

IL-10 Interleukin 10

IL-17 Interleukin 17

Lam Laminin

MEM Minimum essential medium

MMP Matrix metalloproteinases

MRI Magnetic resonance imaging

MSC Mesenchymal stem cells

NGF Nerve growth factor

NMDA N-methyl-d-aspartic acid

NPC Neural progenitor cells

NSC Neural stem cells

NT-3 Neurotrophin-3

OGD Oxygen-glucose deprivation

ORO Oil Red O

PBS Phosphate buffered saline

pCN Primary cortical neuronal cells

PDL Poly-D-lysine

PFA Paraformaldehyde

PI Propidium iodide

PLO Poly-L-ornithine

PPARγ Peroxisome proliferator-activated receptor gamma

ROS Reactive oxygen species

rtPA Recombinant tissue plasminogen activator

SDF-1 Stromal cell-derived factor 1

SEM Standard error of the mean

shRNA Short hairpin RNA

TNFα Tumour necrosis factor alpha

VEGF Vascular endothelial growth factor

α-MEM Alpha-modified minimum essential medium

Abstract

Background: Ischaemic stroke is a severe condition which can be defined as a neurological deficit of vascular origin. The disease is a major cause of permanent disability and is ranked as the second leading cause of death worldwide. Current therapies are unable to sufficiently improve functional outcome in patients. Stem cell therapy is considered as a promising treatment strategy that aims to reduce neuronal damage and stimulate host repair. The goal of this study is to characterize the neuroprotective and neuroregenerative effects of human dental pulp stem cells (DPSC) *in vitro* and identify key paracrine factors responsible for these effects.

Materials & Methods: The neuroprotective capacity of DPSC and key paracrine factors was evaluated by performing an oxygen-glucose deprivation (OGD) survival assay on primary cortical neuronal cells (pCN). OGD-exposed pCN were incubated with conditioned medium of DPSC (CM-DPSC) or with various concentrations of neurotrophic factors for 24 h, after which neuronal survival/death was determined. The neuroregenerative effects of DPSC and multiple growth factors were assessed by investigating the effect of CM-DPSC and paracrine factors on neural stem cell (NSC) migration via a transwell migration assay.

Results: Addition of CM-DPSC and different concentrations of key neurotrophic factors post OGD has no significant effect on neuronal survival after 3 h and 6 h of OGD compared to control medium. In accordance, no improvement in neuronal viability is observed after 3 h and 6 h of OGD following incubation of pCN with CM-DPSC and various concentrations of paracrine factors during the OGD conditions. Furthermore, CM-DPSC significantly promotes NSC migration compared to CM of human dermal fibroblasts (HDF) and control medium. Although not significant, CM-DPSC seems to have a higher migratory effect on NSC than CM of bone marrow-derived mesenchymal stem cells (BM-MSC). Additionally, NSC migration is significantly enhanced by insulin-like growth factor II (IGF-II) and stromal cell-derived factor 1 (SDF-1) compared to control.

Discussion & Conclusion: The present study demonstrates that CM-DPSC and key paracrine factors do not significantly enhance neuronal survival after OGD. This could be due to the extended OGD exposure time, which might possibly induce irreversible damage in pCN. Alternatively, other assays such as glutamate excitotoxicity could be explored for future neuroprotection studies. In contrast, CM-DPSC significantly promotes NSC migration, which suggests potential beneficial effects of DPSC on endogenous neuroregeneration. Moreover, we show that IGF-II and SDF-1 have a significant migratory effect on NSC. Hence, these two factors represent interesting key paracrine factors which could possibly be responsible for DPSC-mediated NSC migration. In conclusion, this study offers evidence for the neuroregenerative capacity of DPSC *in vitro*. However, more elaborate research on the *in vitro* neurorestorative effects of DPSC has to be performed to gain insight in the therapeutic potential of DPSC in ischaemic stroke.

Samenvatting

Inleiding: Een ischemisch herseninfarct is een ernstige aandoening dat gedefinieerd wordt als een neurologisch deficit van vasculair origine. De ziekte is één van de belangrijkste oorzaken van permanente invaliditeit en wordt gerangschikt als de tweede grootste doodsoorzaak ter wereld. De huidige therapieën zijn niet in staat om het functionele herstel van patiënten voldoende te verbeteren. Stamceltherapie wordt beschouwd als een veelbelovende therapeutische strategie om neuronale schade te verminderen en endogene herstel mechanismen te stimuleren. Het doel van dit onderzoek is om de neuroprotectieve en neuroregeneratieve effecten van humane dentale pulpa stamcellen (DPSC) *in vitro* te karakteriseren en om de belangrijkste paracriene factoren verantwoordelijk voor deze effecten te identificeren.

Materiaal & Methoden: De neuroprotectieve capaciteit van DPSC en belangrijke paracriene factoren werd geëvalueerd aan de hand van een zuurstof-glucose deprivatie (OGD) assay die uitgevoerd werd op primaire corticale neuronale cellen (pCN). OGD-blootgestelde pCN werden geïncubeerd met geconditioneerd medium van DPSC (CM-DPSC) of met verschillende concentraties van 3 neurotrofe factoren voor 24 h, waarna neuronale cel viabiliteit/dood werd bepaald. De neuroregeneratieve effecten van DPSC en verscheidene groeifactoren werden beoordeeld door het effect van CM-DPSC en paracriene factoren op neurale stamcel (NSC) migratie te onderzoeken via een transwell migratie assay.

Resultaten: Toevoeging van CM-DPSC en verschillende concentraties van 3 neurotrofe factoren post OGD heeft geen significant effect op neuronale overleving na 3 h en 6 h OGD in vergelijking met controle medium. In overeenstemming, incubatie van pCN met CM-DPSC en variërende concentraties van de paracriene factoren tijdens OGD condities is niet in staat om neuronale viabiliteit te verbeteren na 3 h en 6 h OGD. Bovendien, CM-DPSC bevordert significant NSC migratie vergeleken met CM van humane dermale fibroblasten (HDF) en controle medium. Hoewel niet significant, CM-DPSC blijkt een groter effect te hebben op NSC migratie dan CM van beenmerg mesenchymale stamcellen (BM-MSC). Bijkomend, NSC migratie is significant verhoogd door insulin-like growth factor II (IGF-II) en stromal cell-derived factor 1 (SDF-1) in vergelijking met controle medium.

Discussie & Conclusie: De huidige studie toont aan dat CM-DPSC en belangrijke paracriene factoren niet in staat zijn om significant neuronale viabiliteit te verhogen na OGD. Dit kan gelegen hebben aan de ruime OGD blootstelling tijd, dat mogelijks irreversibele schade geïnduceerd heeft in pCN. Alternatief, andere assays zoals glutamaat excitotoxiciteit kunnen uitgetest worden voor verdere neuroprotectie experimenten. Daarentegen, CM-DPSC bevordert significant NSC migratie, wat potentiele voordelige effecten suggereert van DPSC op endogene neuroregeneratie. Daarnaast hebben we aangetoond dat IGF-II en SDF-1 NSC migratie stimuleren. Bijgevolg worden deze 2 factoren beschouwd als interessante paracriene factoren die mogelijks verantwoordelijk kunnen zijn voor DPSC gemedieerde NSC migratie. In conclusie, deze studie levert bewijs voor de neuroregeneratieve capaciteit van DPSC *in vitro*. Echter, bijkomend onderzoek moet verricht worden om inzicht te verwerven in het therapeutisch potentieel van DPSC in herseninfarcten.

1 Introduction

Ischaemic stroke can be defined as a focal **neurological deficit of vascular origin** with a sudden onset and rapid occurrence of symptoms. The disease is one of the most devastating neurological disorders since it is a major cause of permanent disability in patients [1]. Worldwide, ischaemic stroke is ranked as the second leading cause of death, accounting for 5.9 million deaths annually. The global incidence of stroke ranges from 240 to 600 per 100.000 people, which corresponds to 16.9 million incident stroke cases per year [1, 2]. Approximately 6% of total health care budgets is spent on stroke management, which means that this disease poses a major burden on health care systems [3, 4]. Since stroke is a disease of aging, the prevalence and socioeconomic burden of stroke will continue to rise, given that the number of individuals over the age of 65 will double by 2030 [1, 2].
Stroke can be divided into **two subtypes**; ischaemic stroke and haemorrhagic stroke. Ischaemic stroke is the most common type, comprising approximately 80% of all stroke cases [4]. The causes of ischaemia can be classified into five categories: thrombosis, embolism, systemic hypoperfusion, venous congestion, and arterial luminal obliteration. In most cases, thrombotic or embolic occlusion of a large cerebral artery is the underlying cause of the ischaemic insult [5]. Current therapies mainly focus on restoring perfusion via thrombolysis [4, 6]. However, this therapeutic strategy is unable to sufficiently improve the disease outcome and is only applicable in 4% of the patients due to several contraindications as will be discussed below [6]. Therefore, there is an **urgent need for more effective therapies** that promote functional recovery in stroke patients.

1.1 Pathophysiology of ischaemic stroke

At the start of the ischaemic event, blood flow to certain brain areas is impaired due to a vascular deficiency (e.g. thrombosis, embolism, etc.) [5]. As a consequence, brain tissue near the affected vessel is deprived of oxygen and essential nutrients, which induces irreversible damage in the afflicted region. This area of lethally damaged tissue is called the **ischaemic core**. However, the area surrounding the core, called the **penumbra**, consists of viable brain tissue that is functionally impaired [5, 7]. In the penumbra, the survival of individual cells depends mainly on the duration of ischaemia, the degree of ischaemia and the amount of collateral blood flow toward this area. Therefore, the penumbra can be regarded as an area "at risk" that still has the potential to be rescued. Hence, this area is considered to be the main target for therapeutic interventions in stroke [7].

In the ischaemic core and penumbra, a serie of neurochemical events occurs, also referred to as the **ischaemic cascade** [7]. The brain requires a high amount of oxygen and glucose as an energy source, which is important to assure normal cell function and maintain ionic homeostasis. Impairment of cerebral blood flow causes disturbances in these vital energetic processes [8]. Ischaemia leads to the dysfunction of ATP-dependent ion pumps, such as the Na^+/K^+ pump, which results in loss of membrane potential and depolarisation of neuronal and glial cells [4]. Subsequently, voltage-dependent Ca^{2+} channels are activated and excitatory neurotransmitters, including glutamate, are released into the extracellular space. Accumulation of glutamate in the

extracellular space leads to the stimulation of α-amino-3-hydroxy-5-methyl-4-isoxazole propionic acid (AMPA) and N-methyl-d-aspartic acid (NMDA)-type glutamate receptors on adjacent neurons. Consequently, these neurons become depolarized, which results in additional calcium influx and glutamate release, causing an exacerbation of the initial ischaemic insult. Due to the ionic imbalance, intracellular fluid accumulation occurs, which is responsible for the formation of cytotoxic oedema [7, 8]. Furthermore, the increase in intracellular Ca^{2+} leads to the activation of Ca^{2+}-dependent enzymes, such as proteases, endonucleases, phospholipases and cyclooxygenases. These enzymes cause extensive cell damage and are partially responsible for the generation of reactive oxygen species (ROS). ROS are important mediators of cellular damage by inducing DNA damage, lipid peroxidation and protein denaturation, which ultimately results in mitochondrial failure and membrane disruption [4, 7, 8]. The end result of these molecular events is **acute cell death** via necrosis or apoptosis, depending on the degree of ischaemic injury [4, 9].

Besides inducing cellular damage, ROS production is responsible for blood-brain barrier (BBB) dysfunction through endothelial cell damage and activation of matrix metalloproteinases (MMP) [4, 7]. Moreover, necrotic cells release a plethora of inflammatory cytokines that activate resident microglia and stimulate the infiltration of neutrophils and monocytes in the lesion. The factors (inflammatory cytokines, ROS, etc.) produced by these activated immune cells further amplify the ischaemic cascade of tissue damage and cause additional BBB disruption [4, 7, 10]. Because of the complex events that are involved at the start of the ischaemic event, multiple therapeutic strategies have been considered that target molecular processes in the ischaemic cascade. However, these experimental drugs often failed in clinical trials because of the relative short therapeutic administration window of these agents and the multiplicity of biochemical events involved [11, 12].

1.2 Current therapies for ischaemic stroke and their limitations

Current therapies mainly focus on saving the penumbra by restoring perfusion via recanalization of the occluded vessel. Recanalization can be achieved via **thrombolysis** with **recombinant tissue plasminogen activator (rtPA)**, which is currently the standard pharmacological treatment for stroke approved by the Food and Drug Administration (FDA) [6, 10]. Although this approach has proven to reduce stroke-related mortality, rtPA-therapy has several **limitations**. First of all, rtPA can only be administered within 4.5 hours of stroke onset. Beyond these 4.5 hours, the risk of intracerebral haemorrhage outweighs the benefits. Due to this narrow therapeutic time frame, rtPA treatment is only applicable in 4% of the patients [6]. Moreover, patients are commonly admitted to the hospital with advanced symptoms and are mostly diagnosed with a delay of two hours, thereby often exceeding the safe treatment window of 4.5 hours [13]. In addition, rtPA therapy is unable to significantly improve functional outcome, since the reperfusion process can lead to secondary tissue damage [14]. Other recanalization techniques, such as aspirin administration, thrombectomy and stenting, are clinically available. Although a high rate of recanalization can be achieved with these approaches, they can only be initiated within the first hours after stroke onset and do not provide a superior outcome to rtPA-therapy [6, 11]. Since modern medicine is unable to sufficiently improve functional recovery in patients, there is an urgent need for more effective

therapies for stroke. New treatment strategies should aim at preventing neuronal damage and restoring lost neural tissue in addition to reperfusion [11, 15].

1.3 Stem cells: a tool for regenerative medicine

The use of stem cells in research has increased significantly over the last decades. Cell-based therapies represent an interesting tool for regenerative medicine, based on the stem cells' ability to replace or enhance repair of damaged tissues. **Stem cells** can be defined as cells with the capacity to self-renew and differentiate into more specialized cells [16-18]. In the adult organism, a pool of stem cells is present in various organs and tissues. These stem cells are responsible for natural tissue turnover and reconstitution of damaged tissue. Adult stem cells are often referred to as multipotent stem cells, since they are able to differentiate into different cell types of exclusively one germ layer. In addition to multipotent stem cells, unipotent or progenitor stem cells can be found in several adult tissues. In contrast to other stem cell types, these cells are able to differentiate into only one specified cell type. Based on their location within the body, several types of adult stem cells can be identified. The three most characterized cell types are haematopoietic stem cells, neural stem cells and mesenchymal stem cells [16]. **Mesenchymal stem cells (MSC)** have been extensively studied in recent years and can be found in several tissues, such as the bone marrow, adipose tissue, dental pulp tissue, umbilical cord blood and placenta. Several criteria are used to identify cells as MSC. First of all, they have to possess the capacity to differentiate into osteoblasts, chondroblasts and adipoblasts. Moreover, the cells should be able to adhere to plastic and express a panel of defined cell surface markers. By definition, MSC should express CD73, CD105 and CD90, whereas they should lack the expression of CD11b, CD14, CD34, CD45, CD19 and HLA-DR. Other characteristics of MSC include a high proliferation capacity and immunomodulatory properties [19]. In addition to their multilineage differentiation potential toward mesodermal cell lineages, MSC are able to (trans)differentiate into cell types of other germ lineages (neural cells, hepatocytes, epithelial cells, etc.) [20, 21].

In 2000, the group of Gronthos et al. identified a new stem cell source present in dental pulp tissue, referred to as **human dental pulp stem cells (DPSC)**. DPSC form a heterogeneous, clonogenic cell population, which can be isolated from pulpal tissue of molars. Within each colony, individual cells can be characterized by a fibroblast-like morphology [22]. In general, it is suggested that DPSC originate from migrating neural crest cells [23]. Despite their neuro-ectodermal origin, DPSC possess various MSC characteristics, such as the capacity of mesodermal multilineage differentiation, plastic-adherence and expression of mesenchymal stem cell markers. DPSC are positive for the surface markers CD29, CD44, CD59, CD73, CD90, CD105, CD106 and CD146, while being negative for CD11b, CD19, CD34 and CD45. In addition to their osteogenic, adipogenic and chondrogenic differentiation potential, DPSC are able to (trans)differentiate into neural cells, such as neurons and astrocytes [22, 24-27].

DPSC represent an interesting stem cell source for cell-based therapies in various pathological conditions. A great advantage of DPSC is that the **isolation procedure** is performed in a minimal invasive manner and is associated with **low donor site morbidity** [28]. Furthermore, DPSC exhibit immunomodulatory characteristics, possess a high *ex vivo* proliferation capacity [22, 29],

and retain their stem cell properties after long-term cryopreservation, which makes them suitable for future application in patients [30]. The main focus for the use of DPSC in cell-based therapies is on the regeneration and reconstruction of dental structures. DPSC consist of a high dentinogenic differentiation potential and have shown to generate dentin-pulp-like structures *in vivo* [22, 24]. In addition to tooth regeneration, DPSC can have several applications in other domains. For example, DPSC can be of value as cell-based therapy in several bone-related diseases, due to their osteoregenerative capacity [31]. Additionally, DPSC possess **angiogenic properties** and have shown to be beneficial in animal models for myocardial infarction [32, 33]. Furthermore, their **neuro-ectodermal origin and neurogenic properties** (e.g. expression of neurogenic markers, secretion of neurotrophic factors, etc.) suggest the potential use of these stem cells as cell-based therapies in neurological disorders [34-36].

1.4 Stem cell therapy in ischaemic stroke

As mentioned earlier, the **current treatment** concept for ischaemic stroke is **confined to systemic or local thrombolysis** in the acute phase, which is unable to improve disease outcome in stroke patients. From a therapeutic viewpoint, there is an urgent need for more effective treatment strategies. **Stem cell therapy** is considered as a new interesting approach in the treatment of stroke, since this approach aims to **reduce neuronal damage** by influencing local repair mechanisms in the acute and chronic phase of the ischaemic insult [17, 37]. Several preclinical and clinical studies have been performed showing beneficial effects of stem cell therapy on functional recovery [10, 38]. However, little is known about the exact mechanism of action and the optimal treatment protocol of stem cells in stroke. In order to develop an effective cell-based therapy, it is important to exploit the ideal stem cell source. Initially, neural stem cells (NSC) derived from foetal or adult brains were considered to be ideal candidates for cell-based stroke therapies because of their neurogenic differentiation potential [17, 39]. However, due to ethical concerns with foetal cells and isolation difficulties with adult NSC, alternative stem cells sources have been explored, including MSC from various tissues [40].

1.4.1 Potential mode of actions of cell-based therapies in stroke

Multiple mechanisms of action have been proposed for the beneficial effects of cell-based therapies in stroke (Fig 1). The main mechanisms include neuronal replacement, neuroprotection, stimulation of endogenous neuroregeneration, stimulation of angiogenesis and immunomodulation [10, 41]. By definition, stem cells should be able to reconstitute lost neural tissue via **(trans)differentiation toward neural cells** [42]. MSC have been successfully differentiated into neuronal cells with functional characteristics *in vitro* [27, 43]. Moreover, several studies have confirmed that MSC are able to differentiate in neural cells *in vivo* and integrate into the host brain after transplantation in stroke animal models [10, 44]. Despite the encouraging results in this field, neuronal integration seems to be too limited and therefore is not considered to be the main mechanism for an improved outcome after stroke [45]. Recently, it is thought that the beneficial effects of stem cell therapy in stroke models are mainly derived from **paracrine factors** secreted by stem cells [37, 46]. The rich secretome of stem cells consists of a variety of growth factors, including several neurotrophic factors such as nerve growth factor (NGF), brain-derived neurotrophic factor (BDNF) and glial cell-

derived neurotrophic factor (GDNF). Stem cells can be considered as a growth factor delivery vehicle, which can influence the local environment within the stroke lesion. By secreting neurotrophic factors, stem cells can provide trophic support to damaged neuronal cells present in the penumbra. In this way, the stem cells' secretome can exert **neuroprotective effects** and rescue damaged neuronal cells from cell death in the acute phase, thereby preventing additional neuronal damage [37, 41]. In addition to neuroprotection, the secreted trophic factors can also **stimulate endogenous repair mechanisms**. The recruitment of NSC to the stroke lesion represents an important source of endogenous neuroregeneration. In the adult human brain, NSC are predominantly located in the subventricular zone and the subgranular zone of the dentate gyrus [17]. After cerebral ischaemia, NSC migrate toward the injury site via the SDF-1/CXCR-4 axis and contribute to brain repair via differentiation into neurons and integration in the circuitry [17, 47]. Stromal cell derived factor 1 (SDF-1) has been shown to be upregulated at the lesion site and induces the recruitment of NSC toward the injury [47, 48]. Unfortunately, this endogenous regeneration mediated by NSC is insufficient in the adult brain. Therefore, stem cell therapy is an interesting approach to stimulate and improve the recruitment of endogenous NSC to the stroke lesion via delivery of growth factors such as SDF-1 [49, 50]. Another important mechanism of stem cell therapy is stimulating the formation and attraction of new blood vessels toward the stroke lesion. This process is called **angiogenesis** and is mediated via the secretion of several proangiogenic factors such as vascular endothelial growth factor (VEGF) [51]. An emerging concept in stroke research is stem cell-mediated **immunomodulation**. The immunomodulatory properties of MSC can be used to dampen immune responses at the infarct zone. Ischaemic stroke is characterized by infiltration of neutrophils and leukocytes in the lesion, which results in a strong inflammatory response [41]. Due to their immunosuppressive characteristics, it has been demonstrated that MSC are able to reduce levels of pro-inflammatory cytokines, such as IL-17, IL-1β and TNFα, while increasing the expression of anti-inflammatory markers like IL-10. Furthermore, transplanted MSC have shown to inhibit T cell proliferation, diminish macrophage/monocyte infiltration, reduce the activation of neutrophils and promote T regulatory cell expression within the stroke lesion [41, 52].

Despite the great preclinical promise of stem cell therapy in ischaemic stroke, the **optimal administration route and fate** of the donor cells remain largely **unknown**. To gain insight into the behaviour and distribution of the transplanted stem cells in the host, several non-invasive imaging methods can be used. Examples of these imaging methods include magnetic resonance imaging (MRI) and bioluminescence imaging (BLI) [53, 54]. The latter involves labelling of stem cells with a reporter gene such as firefly luciferase (fluc), which can be detected via a light-emitting reaction. This method is a highly sensitive technique to monitor cell migration and survival. In addition, imaging methods like MRI can provide information on morphological adaptations in the host brain, such as changes in lesion volume and revascularisation. Combining these imaging methods will provide more insight into the fate of donor cells by correlating the localization of transplanted cells with morphological changes at the injury site [10].

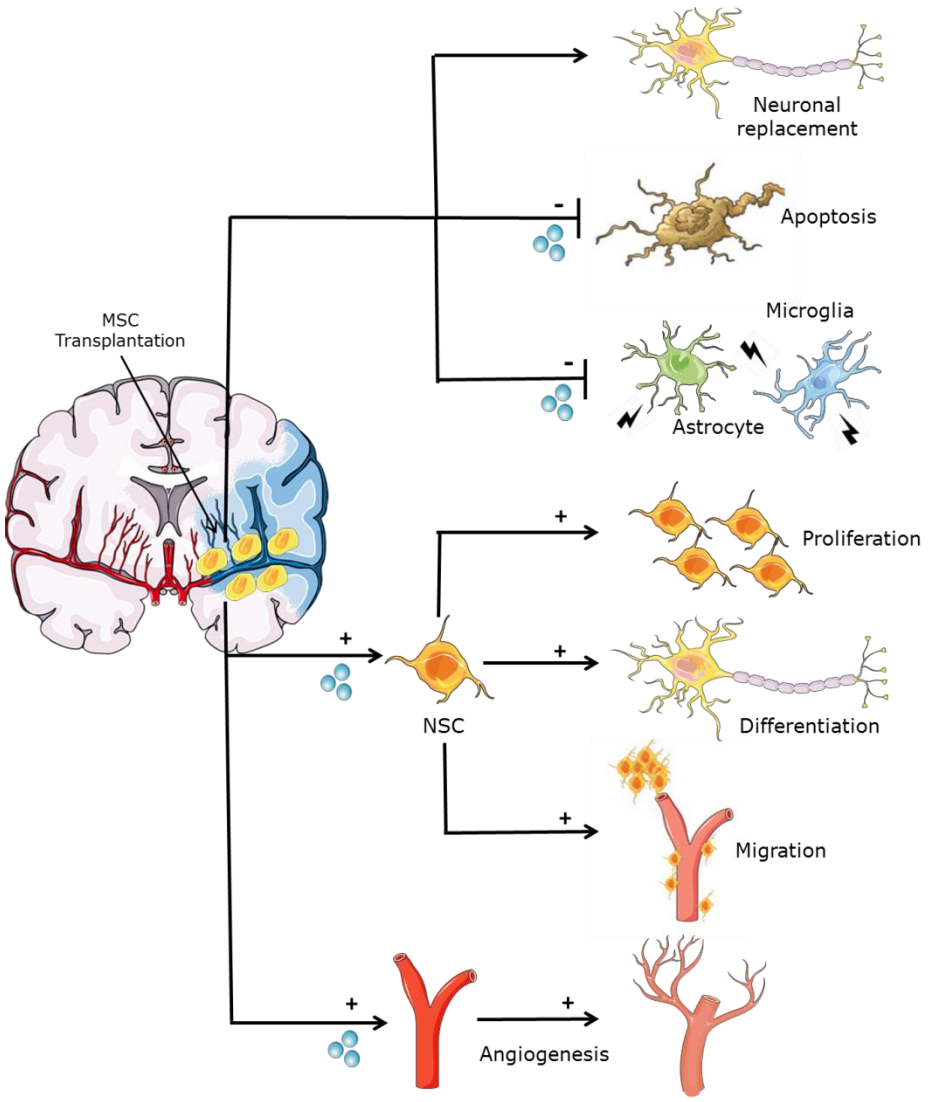

Figure 1: Proposed mechanism of actions of MSC-based therapies in ischaemic stroke. Transplantation of MSC can modulate the local microenvironment in the stroke lesion by stimulating neural repair via multiple mechanisms: neuronal replacement, neuroprotection, stimulation of endogenous neuroregeneration (including NSC proliferation, migration and differentiation), stimulation of angiogenesis and immunomodulation. These beneficial effects are mainly mediated by paracrine factors secreted by the stem cells, although cell–cell interactions may also play a role. Figure was created using Servier Medical Art. MSC: mesenchymal stem cells; NSC: neural stem cells.

1.4.2 The use of DPSC as cell-based therapy in stroke

The present study focuses on the application of DPSC as a cell-based stroke therapy. DPSC are considered to be favourable candidates for stem cell therapy in various neurological disorders. Several comparative studies have demonstrated that DPSC show a higher proliferation and immunomodulatory capacity than the classical bone marrow-derived MSC (BM-MSC) [22, 29]. Moreover, DPSC display more neuroprotective effects and secrete higher amounts of neurotrophic factors compared to BM-MSC [55, 56].

Recently, DPSC have gained increased interest by researchers due to their neurogenic properties. DPSC express basal levels of **neurogenic markers** and are known to **secrete several neurotrophic factors**, including NGF, neurotrophin-3 (NT-3), BDNF and GDNF [34-36].

Furthermore, DPSC are able to induce endogenous axon guidance within a host nervous system and promote the proliferation and differentiation of neural progenitor cells (NPC) *in vivo* [57, 58]. In *in vitro* models of Alzheimer's and Parkinson's disease, DPSC have shown to enhance the survival of hippocampal and dopaminergic neurons exposed to neurotoxins [35, 59]. These neuroprotective effects are thought to be mediated by neurotrophins produced by the DPSC. Moreover, DPSC have been able to promote neurite outgrowth in trigeminal neurons and rescue motor neurons in spinal cord injury models by providing neurotrophic support [36].

Preclinical studies have demonstrated that DPSC transplantation improves functional recovery and lesion severity in stroke animal models [45, 60, 61]. However, the exact mechanism of neural repair has yet to be elucidated. Former research has mainly focused on the cellular integration of transplanted DPSC in the stroke lesion. Nevertheless, minimal neuronal replacement is found within the peri-infarct region [45, 61]. Increasing evidence suggests that **paracrine factors** secreted by DPSC play important roles in promoting functional recovery following stroke [45, 56, 61]. Song et al. demonstrated that conditioned medium of DPSC (CM-DPSC) confers neuroprotection to ischaemic astrocytes and reduces ischaemia-induced astrogliosis in an *in vitro* model for ischaemic stroke [56]. Moreover, other studies suggested that transplanted DPSC support the recruitment of NPC toward the infarct zone via paracrine effects, thereby promoting endogenous neurogenesis [61]. Although very promising results have been observed in experimental stroke models, further research is needed to understand the underlying mechanisms of action of DPSC following transplantation.

1.5 Research aims

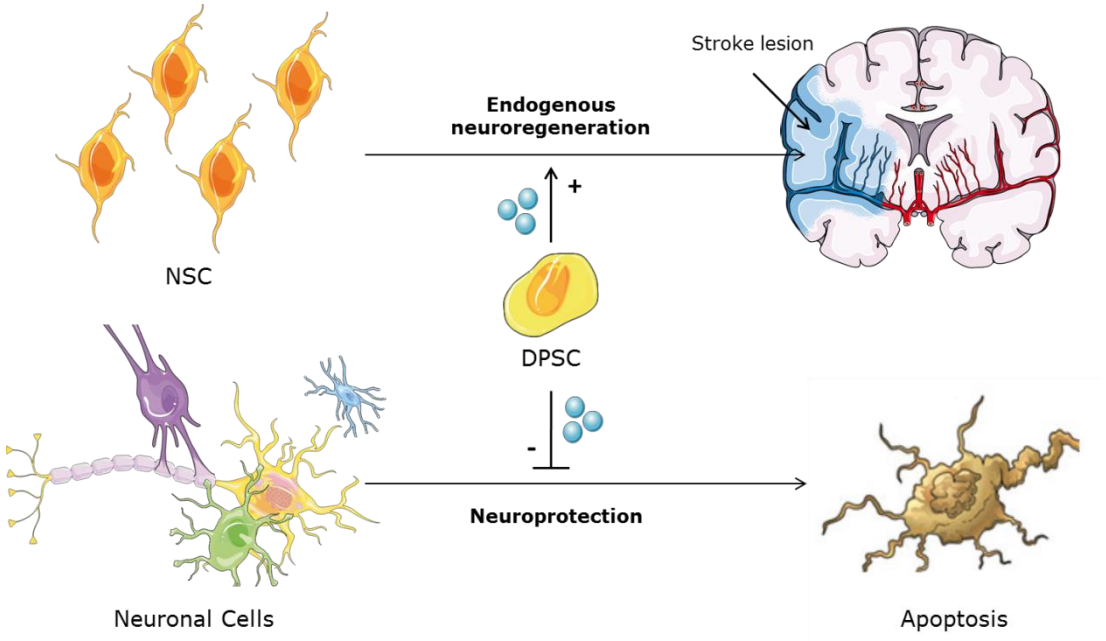

Figure 2: Schematic overview of the research objectives. The goal of this study is to identify potential neuroprotective and neuroregenerative effects of DPSC *in vitro*. The neuroregenerative capacity of the DPSC secretome is evaluated by assessing the effect of CM-DPSC on NSC migration. Furthermore, the ability of CM-DPSC to promote the survival of ischaemic neuronal cells is investigated. Figure was created using Servier Medical Art. DPSC: dental pulp stem cells; NSC: neural stem cells.

The aim of this study is to characterize the neurorestorative role of the DPSC secretome in post-stroke repair. Our **hypothesis** is that paracrine factors produced by DPSC enhance neural repair via **neuroprotection** and **stimulation of endogenous neuroregeneration**. In this study, the ability of the DPSC secretome to promote the survival of neuronal cells exposed to ischaemic conditions is determined. To assess the neuroprotective effects of DPSC, an oxygen-glucose deprivation (OGD) neuronal survival assay is performed. In this assay, primary cortical neuronal cells (pCN) are exposed to oxygen and glucose deprivation. Subsequently, the effect of CM-DPSC on neuronal survival is assessed. Additionally, the key paracrine factor(s) responsible for neuronal survival are identified. Based on a growth factor array performed on CM of DPSC (see Fig 8), three paracrine factors are selected, which are considered to play important roles in the neuroprotective capacity of DPSC. These three paracrine factors include BDNF, GDNF, and insulin-like growth factor II (IGF-II). The aim is to evaluate which of these single factors is most potent in enhancing neuronal survival by performing an OGD-neuronal survival assay as explained above. The ultimate goal is to upregulate this paracrine factor in DPSC via lentiviral transduction to boost the neuroprotective effects of DPSC.

To assess the capacity of DPSC to promote neurogenesis, the effect of the DPSC secretome on NSC migration is examined. The migration of NSC in response to CM-DPSC is evaluated by means of a transwell migration assay. Furthermore, the neuroregenerative properties of several neurotrophic factors (BDNF, GDNF, NGF, NT-3 and IGF-II) are screened via this transwell system. The results of this assay will be used to identify the key paracrine factor responsible for NSC migration, which can be incorporated in the lentiviral vector. The findings obtained from this study will provide more insight into the paracrine effects of DPSC and their potential mechanism of action in neuronal repair. This can give us crucial information on the therapeutic potential of DPSC in stroke, which ultimately can be translated into a new effective stem cell-based therapy for ischaemic stroke.

2 Materials and methods

2.1 Isolation and culture of human dental pulp stem cells

DPSC were obtained from third molars extracted for orthodontic reasons at Ziekenhuis Oost-Limburg (Genk, Belgium). Informed consent was given by the donor or legal guardian in the case of underaged patients (< 18 years). The age of the donors varied from 15 to 25 years old. Experiments performed in this study were approved by the Medical Ethical Committee of Hasselt University (13/0104U). To obtain dental pulp tissue, third molars were mechanically fractured to expose the pulp cavity. DPSC were isolated from the pulpal tissue by means of the explant methodology. Dental pulp tissue was collected using forceps and the tissue was rinsed in alpha-modified minimum essential medium (α-MEM) (Sigma-Aldrich, St. Louis, United states of America) supplemented with 2 mM L-glutamine (Sigma-Aldrich), 10% foetal bovine serum (FBS) (Gibco, Paisley, United Kingdom), 100 U/ml penicillin and 100 µg/ml streptomycin (Sigma-Aldrich). The dental pulp tissue was cut into small pieces, which were cultured in six-well plates at 37°C and 5% CO_2 to allow DPSC outgrowth of the tissue. Culture medium was changed every 3–4 days. The cell culture was evaluated daily using the Nikon Eclipse TS100 inverted phase contrast microscope (Nikon, Tokyo, Japan). When 70-80% confluence was reached, the DPSC were harvested using 0.05% trypsin/EDTA (Sigma-Aldrich). Subsequently, the cell suspension was centrifuged (300 g, 6 min) and viable cells were counted via trypan blue exclusion (Sigma-Aldrich). For sub-culturing, DPSC were seeded at a density of 4 x 10^3 cells/cm^2. DPSC from passage 2 to 8 were used in all experiments. For cryopreservation, α-MEM supplemented with 10% dimethyl sulfoxide (DMSO, Sigma-Aldrich) and 20% FBS was applied.

2.2 Culture of human dermal fibroblasts

Human dermal fibroblasts (HDF) were purchased from Sigma-Aldrich and cultured in Dulbecco's modified Eagle's medium (DMEM, Sigma-Aldrich), supplemented with 10% FBS, 100 U/ml penicillin and 100 µg/ml streptomycin. Throughout this study, HDF from passage 2 to 9 were used. In short, HDF were passaged using 0.05% trypsin/EDTA when 70-80% confluence was reached. HDF were seeded in culture flasks at a density of 3 x 10^3 cells/cm^2. The cell culture was monitored daily with the Nikon Eclipse TS100 inverted phase contrast microscope and fresh medium was added to the cell culture every 3 days. For cryopreservation, HDF were resuspended in DMEM supplemented with 20% FBS and 10% DMSO.

2.3 Culture of bone marrow-derived mesenchymal stem cells

Human BM-MSC were kindly provided by Prof. C. Verfaillie (Stem cell institute, KULeuven, Leuven, Belgium). BM-MSC were cultured in DMEM, supplemented with 10% FBS, 100 U/ml penicillin and 100 µg/ml streptomycin. BM-MSC from passage 2 to 9 were used in this study. At 70-80% confluence, BM-MSC were passaged using 0.05% trypsin/EDTA. BM-MSC were seeded at a density of 3 x 10^3 cells/cm^2 in culture flasks for sub-culturing. Medium was changed every 3 days and the cell culture was monitored daily using the Nikon Eclipse TS100 inverted phase contrast microscope. BM-MSC were cryopreserved in DMEM supplemented with 20% FBS and 10% DMSO.

2.4 Production of conditioned medium

For CM production, cells were seeded at a density of 2 x 10^4 cells/cm^2 and cultured for 24 h in standard culture medium to allow cell adherence. After 24 h, cells were washed two times with phosphate buffered saline (PBS, Lonza, Basel, Switzerland) and incubated with α-MEM (0% FBS) supplemented with 2 mM L-glutamine , 100 U/ml penicillin and 100 µg/ml streptomycin. The cells were cultured for 48 h, after which CM was collected. The CM was centrifuged for 8 min at 1500 g and subsequent filtered through a 0.22 µm filter to remove cellular debris. CM was stored at -80°C.

2.5 Isolation and culture of primary cortical neuronal cells

pCN were isolated from mouse embryos at embryonic day 16 to 18 (E16-18) of development. The experiments were approved by the Ethical Committee for animal experiments of Hasselt University (protocol number 201546K). A pregnant C57Bl/6 mouse was sacrificed via cervical dislocation after which the embryos were collected. Subsequently, embryos were decapitated and brains were carefully isolated. Brains were transferred to Hank's balanced salt solution (HBSS, Gibco) supplemented with 7 mM Hepes (Gibco), 100 U/ml penicillin and 100 µg/ml streptomycin. After removal of the meninges, the cortices were dissected under a Leica S6E stereo microscope (Leica microsystems, Wetzlar, Germany). Next, cortices were incubated at 37°C for 15 min with HBSS/Hepes solution supplemented with 0.05% trypsin/EDTA solution (Invitrogen, Merelbeke, Belgium). After washing three times with minimum essential medium (MEM, Gibco) supplemented with 10% horse serum (Gibco), 0.6% glucose, 100 U/ml penicillin and 100 µg/ml streptomycin (referred to as pCN plating medium), cortices were mechanically disrupted via resuspending the tissue with a micropipette. The cell suspension was centrifuged at 300 g for 6 min, after which the cells were resuspended in pCN plating medium. Subsequently, the cell suspension was rinsed through a 70 µm cell strainer (Thermo Fisher Scientific, Erembodegem, Belgium). pCN were seeded at a density of 2.4 x 10^5 cells/cm^2 in high-attachment culture plates (Greiner Bio-one, Wemmel, Belgium) for OGD survival assays. The culture plates were coated with 100 µg/ml poly-L-ornithine (PLO, Sigma-Aldrich). After attachment of pCN to the coated plates, the pCN plating medium was replaced by neurobasal medium (Gibco) supplemented with 2% B27 + vitamin A (Gibco), 2 mM L-glutamine, 100 U/ml penicillin and 100 µg/ml streptomycin. The cells were cultured for at least five days to allow maturation of pCN.

2.6 Oxygen-glucose deprivation neuronal survival assay

For optimization of the surface coating, pCN were cultured at 37°C and 4.6% O_2 in high-attachment culture plates coated with multiple surface coatings. After the maturation period, baseline cell viability was assessed by means of propidium iodide (PI, Sigma-Aldrich) staining. Used surface coatings and concentrations are displayed in table 2. Subsequently, an OGD neuronal survival assay was performed, in which pCN were cultured for 5 h in serum-free DMEM without glucose (Sigma-Aldrich) at 37°C and 0.3% O_2. Neuronal viability was assessed after the OGD conditions via PI staining. Post-OGD, the medium was replaced by α-MEM (0% FBS) and pCN were cultured for 24 h at 2.3% O_2 and 37°C, whereafter neuronal survival was evaluated via PI staining.

For neuroprotection studies, pCN were cultured at 37°C and 4.6% O_2 in high-attachment culture plates coated with 100 µg/ml PLO. Baseline survival values were obtained after the maturation period of 5 days by means of PI staining. To mimic ischaemic conditions, pCN were cultured for 3 h or 6 h in glucose-free DMEM (0% FBS) at 37°C and 0.3% O_2. After the OGD conditions, neuronal survival/death was assessed via PI staining. To investigate neuroprotection, pCN cultures were treated with the experimental conditions during OGD conditions or immediately after OGD (Fig 3). The experimental conditions included CM-DPSC, CM-HDF, CM-BM-MSC or α-MEM (0% FBS) for the assessment of DPSC-mediated neuroprotective effects. To evaluate which paracrine factors play a crucial role in neuroprotection, α-MEM (0% FBS) supplemented with different concentrations of GDNF (2 – 10 - 50 ng/ml), BDNF (20 - 100 - 500 ng/ml) and IGF-II (20 – 100 - 500 ng/ml) (all growth factors; ImmunoTools, Friesoyhte, Germany) was used. However, for the treatment protocol during OGD, the various concentrations of GDNF, BDNF and IGF-II were prepared in glucose-free DMEM and added to the pCN just before OGD induction. After the OGD conditions, medium was replaced by α-MEM (0% FBS) supplemented with the different growth factor concentrations. Next, pCN were cultured for 24 h at 2.3% O_2 and 37°C, after which neuronal survival/death was evaluated using PI staining. To assess neuronal viability, PI staining was performed by adding lysis buffer A100 (Chemometec, Allerod, Denmark), stabilization buffer B (Chemometec) and PI solution (1/100) to the pCN cultures. Neuronal death was evaluated via PI staining (1/100) without addition of lysis and stabilization buffers. After incubation for 15 min at room temperature, fluorescence intensity (FI) was measured at 612 nm using a FLUOstar omega microplate reader (BMG Labtech, Temse, Belgium) with excitation at 540 nm and gain of 2000.

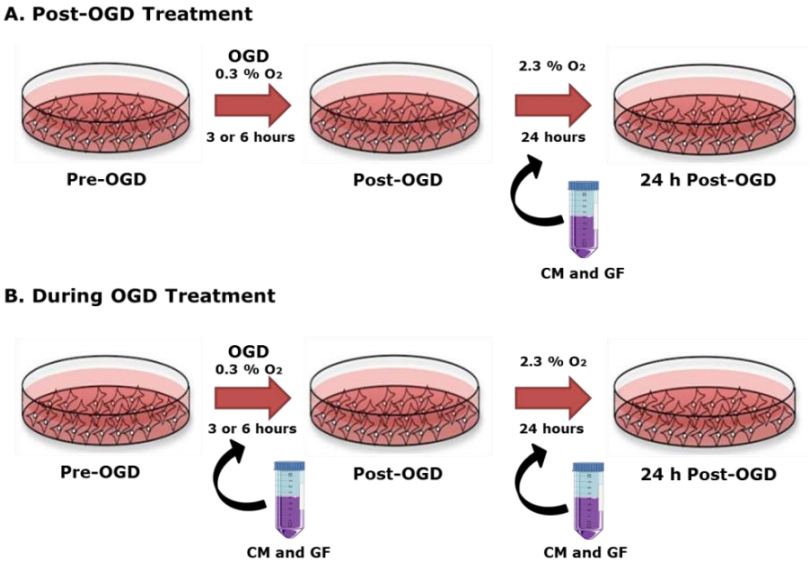

Figure 3: Illustration of the experimental setup of the OGD treatment protocols. (A) Post-OGD treatment protocol. pCN were cultured for 3 h or 6 h on DMEM no glucose and 0.3% O_2. After OGD, pCN were exposed for 24 h to different concentrations of growth factors (diluted in α-MEM) or CM of DPSC, HDF and BM-MSC. **(B)** Treatment protocol during OGD. pCN were cultured under OGD conditions for 3 h or 6 h. However, growth factors (prepared in DMEM no glucose) and CM were added just before OGD. After OGD, the medium was changed and replaced by growth factors and CM, both prepared in α-MEM. In both treatment protocols, baseline neuronal survival/death was assessed before the start of OGD (T0) to which all obtained fluorescence data were normalized. OGD: oxygen-glucose deprivation; CM: conditioned medium; GF: growth factors

2.7 Isolation and culture of neural stem cells

NSC were isolated from mouse embryos on day 15 of embryonic development. Approval for the experiments was given by the Ethical Committee for animal experiments of Hasselt University (protocol number 201546K). A pregnant C57Bl/6 mouse was sacrificed by means of cervical dislocation, after which embryos were isolated and decapitated. The brains of the embryos were carefully dissected and kept in cold PBS supplemented with 100 U/ml penicillin and 100 µg/ml streptomycin. Subsequently, the brains were cut into small fragments and centrifuged for 8 min at 200 g. The fragments were incubated for 90 min at 37°C with PBS supplemented with 2 mg/ml collagenase A (Roche, Vilvoorde, Belgium) and 10 µg/ml DNase I (Sigma-Aldrich). Next, the brain fragments were centrifuged for 5 min at 300 g and the pellet was resuspended in Neurobasal A medium (Gibco). After repetition of the latter step, the cell suspension was centrifuged for 5 min at 300 g and resuspended in Neurobasal A medium supplemented with 1% B27 (without vitamin A, Gibco), 2 mM L-glutamine, 20 ng/ml epidermal growth factor (EGF, ImmunoTools) and 20 ng/ml basic fibroblast growth factor (bFGF, ImmunoTools), 100 U/ml penicillin and 100 µg/ml streptomycin (referred to as standard NSC culture medium). The cell suspension was rinsed through a 70 µm cell strainer and transferred to a T25 flask. Cells were incubated for five days to allow the formation of floating neurospheres. Every two days, EGF and bFGF (both 20 ng/ml) were added to the culture medium. The culture medium containing the free floating neurospheres was collected and centrifuged for 5 min at 270 g. The formed pellets were incubated for 5 min with accutase (Sigma-Aldrich), prior to seeding the NSC at a density of 2 x 10^4 cells/cm^2 in 5 µg/ml fibronectin (R&D Systems, Oxfordshire, United Kingdom) coated culture flasks. The NSC standard culture medium was changed every 3-4 days. The cells were sub-cultured when 80% confluence was reached. For passaging, the cells were incubated for 5 min with accutase and centrifuged for 6 min at 300 g. NSC were seeded at a density of 2 x 10^4 cells/cm^2 in fibronectin coated culture flasks and cultured in standard NSC culture medium. From passage 5 on, NSC were cultured in uncoated flasks. The cells were cryopreserved in STEMdiff Neural Progenitor Freezing Medium (STEMCELL Technologies, Cambridge, United Kingdom).

2.8 Transwell migration assay

Transwell inserts (ThinCert™, 8 µm pore size, Greiner Bio-One) were coated with 5 µg/ml fibronectin overnight at 37°C. Inserts were seeded with NSC (5 x 10^4 cells/insert) resuspended in 150 µl α-MEM (0% FBS) supplemented with 1% B27 (without vitamin A), 2 mM L-glutamine, 100 U/ml penicillin and 100 µg/ml streptomycin, 10 ng/ml EGF and 10 ng/ml bFGF. The lower chemoattractant chamber of the 24-wells plate contained either 500 µl of CM-DPSC, CM-HDF, CM-BM-MSC or 500 µl of BDNF, GDNF, IGF-II, NGF (ImmunoTools) and NT-3 (ImmunoTools) diluted in α-MEM (100 ng/ml for all growth factors). As positive control, α-MEM containing 100 ng/ml SDF-1 (ImmunoTools) was used. All conditions were supplemented with 1% B27 (without vitamin A), 10 ng/ml EGF and 10 ng/ml bFGF. After incubation of 24 h, migrated cells were fixed for 15 min with 4% paraformaldehyde (PFA) and stained with 0.1% crystal violet for 30 min. The membranes were washed with PBS and mounted on coverslips with Aquatex mounting medium (Merck, Darmstadt, Germany). Representative images were taken with the Leica DM2000 light microscope (Leica Microsystems, Leica Application Suite V.4.5. software) and quantified with AxioVision software (Carl

Zeiss, Aalen, Germany). Area percentage was used to quantify the migrated cells present on the membrane.

2.9 Osteogenic differentiation

In vitro differentiation of DPSC, HDF and BM-MSC toward osteogenic cell lineage was performed using the MesenCult™ Osteogenic Stimulatory Kit (STEMCELL Technologies). Cells were seeded on 1 µg/ml fibronectin coated coverslips at a density of 5 x 10^3 cells/cm^2 and incubated until 70-80% confluence was reached. Subsequently, cells were cultured in complete MesenCult™ Osteogenic Stimulatory medium, consisting of MesenCult™ MSC Basal Medium, 15% MesenCult™ Osteogenic Stimulatory Supplements, 0.01 µM dexamethasone and 50 µg/ml ascorbic acid. When multilayering was observed, cells were cultured in complete MesenCult™ Osteogenic Stimulatory medium supplemented with β-glycerophosphate (3.5 mM). Differentiation medium was changed every 3 days. The differentiation process lasted 21 days, after which the osteogenically differentiated cells were fixed in 4% PFA for 20 min. Osteogenic differentiation was assessed via Alizarin Red S staining (to detect calcium nodules) and by immunocytochemical staining for alkaline phosphatase (ALP).

2.10 Adipogenic differentiation

Adipogenic differentiation was induced using the MesenCult™ Adipogenic Differentiation kit (STEMCELL Technologies). DPSC, HDF and BM-MSC were seeded at a density of 5 x 10^3 cells/cm^2 on glass coverslips coated with 1 µg/ml fibronectin. When 90-100% confluency was reached, cells were cultured in complete MesenCult™ Adipogenic Differentiation medium, consisting of MesenCult™ MSC Basal Medium supplemented with MesenCult™ 10x Adipogenic Differentiation Supplement and MesenCult™ 500x Adipogenic Differentiation Supplement. Culture medium was changed every 3 days with complete MesenCult™ Adipogenic Differentiation medium. The differentiation process lasted 21 days. After this period, the adipogenically differentiated cells were fixed with 4% PFA. Adipogenic differentiation was visualized by Oil Red O (ORO) staining (to detect neutral lipids) and via immunocytochemical analysis of fatty acid binding protein 4 (FABP-4).

2.11 Chondrogenic differentiation

For chondrogenic differentiation, a 3D cell pellet culture system was used according to the guidelines provided by the manufacturer (STEMCELL Technologies). DPSC, HDF and BM-MSC were seeded in 15 ml falcon tubes with a density of 5 x 10^5 cells per tube. Complete MesenCult™-ACF Chondrogenic Differentiation Medium was added to the cells, after which cell pellets were generated by centrifugation at 300 g for 8 min. Complete MesenCult™-ACF Chondrogenic Differentiation Medium was prepared using MesenCult™-ACF Chondrogenic Differentiation Basal Medium supplemented with MesenCult™-ACF 20x Chondrogenic Differentiation Supplement. As negative control, pellets of DPSC, HDF and BM-MSC were cultured respectively in α-MEM or DMEM. The differentiation medium was changed every 3 days and the cell pellets were allowed to differentiate for 21 days. Subsequently, the chondrogenic pellets were fixed in 4% PFA for 24 h, embedded in paraffin and 5 µm thick tissue sections were cut using a microtome. To assess chondrogenic differentiation, tissue sections were stained with Alcian Blue (to visualise acidic glycosaminoglycans) and analysed for expression of aggrecan via immunohistochemical stainings.

2.12 Immunocytochemistry

Cells were seeded on uncoated or fibronectin-coated coverslips for immunocytochemical stainings at a density of 5 x 10^3 cells/cm^2. When approximately 50% confluency was reached, cells were fixed with 4% PFA for 20 min. In short, cells were permeabilized with 0.05% Triton (Sigma-Aldrich Aldrich) diluted in PBS (30 min, 4°C) for intracellular stainings. Subsequently, cells were rinsed three times with PBS and nonspecific binding sites were blocked with DAKO protein block (DAKO, Heverlee, Belgium) for 20 min at room temperature. After washing three times with PBS, primary antibodies (diluted in PBS) were incubated for 1 h at room temperature. Control stainings were performed by omitting the primary antibody. Secondary antibodies (diluted in PBS) were incubated for 30 min at room temperature. Unbound primary and secondary antibodies were washed away three times with PBS after each incubation step. The used primary and secondary antibodies in this study are displayed in table 1. Nuclei were stained with 4,6-diamidino-2-phenylindole (DAPI, Invitrogen) for 10 min, followed by three washing cycles with PBS. Next, coverslips were mounted on glass slides with fluorescence mounting medium (Dako, Heverlee, Belgium) for analysis with the Leica DM 4000 BLED fluorescence microscope (Leica Microsystems; Leica Application Suite X software). Images were taken at different magnifications (10 x and 20 x).

Table 1: Overview of antibodies used for immunocytochemical and -histochemical stainings

Target	Host	Conjugate	Dilution	Supplier	Ref nr.
Primary Antibodies					
Aggrecan	Rabbit	/	1/500	Abcam	Ab186414
ALP	Mouse	/	1/50	DSHB	B4-78-S
FABP-4	Rabbit	/	1/125	Abcam	Ab66682
Secondary Antibodies					
Mouse IgG	Donkey	AF488	1/500	Life Technologies	A21202
Rabbit IgG	Donkey	AF555	1/500	Life Technologies	A31572

AF: alexa fluor; ALP: alkaline phosphatase; FABP-4: Fatty acid binding protein 4; DSHB: Developmental Studies Hybridoma Bank, Iowa, United States; Abcam: Cambridge, United Kingdom; Life Technologies: Erembodegem, Belgium

2.13 Immunohistochemistry

Immunohistochemical stainings were performed on tissue sections (5 µm) of the chondrogenic differentiated cell pellets. The paraffin embedded tissue sections were deparaffinised by exposing the sections to xylene and decreasing concentrations of ethanol (100%, 95%, 80%, 70%, 50% ethanol). Antigen retrieval was performed by incubating the sections in heated DAKO citrate buffer (DAKO, 600W) for 10 min. Prior to blocking the nonspecific binding sites with DAKO protein block for 30 min at room temperature, the sections were washed three times with PBS. Primary antibodies were diluted in PBS supplemented with 10% protein block and incubated for 1 h at room temperature. In the control stainings, the primary antibody was omitted. Secondary antibodies, diluted in PBS + 10% protein block, were incubated for 30 min at room temperature. Unbound primary and secondary antibodies were washed away three times with PBS after each incubation step. An overview of the used antibodies is given in table 1. Nuclei were stained with DAPI for 10

min, followed by three PBS washing cycles. Sections were mounted with fluorescence mounting medium for analysis with the Leica DM 4000 BLED fluorescence microscope. Images were taken at different magnifications (10 x and 20 x).

2.14 Histochemical stainings

ORO staining (Sigma-Aldrich, 3 mg/ml) was performed on adipogenically differentiated cells to detect lipid droplets in the cytoplasm. Briefly, cells were incubated for 10 min with ORO, after which the cells were shortly washed with 60% isopropanol, followed by three washing steps with distilled water. To visualize the nuclei, cells were stained with haematoxylin (Merck) for 5 min, whereafter cells were rinsed 3 times with tap water. For the osteogenic differentiation, calcium deposits in the cell cultures were demonstrated using Alizarin Red S. Cell were washed two times with distilled water and subsequently, calcified nodules were stained for 30 min with 40 mM Alizarin Red S solution. Excess Alizarin Red S staining was washed away three times with distilled water, prior to staining nuclei with haematoxylin for 2 min. For the ORO and Alizarin Red S stainings, cells were mounted with Aquatex mounting medium for analysis with the Leica DM2000 light microscope using Leica Application Suite V.4.5. software. Alcian blue staining was used to reveal a ground substance matrix in the chondrogenically differentiated cell pellets. After deparaffinisation and antigen retrieval of the tissue sections, the cell pellets were incubated for 30 min with Alcian Blue. Next, cells were washed three times with tap water and rinsed once with distilled water. Nuclear fast red staining was applied for 10 min to stain cell nuclei. After brief washing with distilled water, Alcian blue stained tissue sections were dehydrated by exposure to increasing concentrations of ethanol (70%, 80%, 95% and 100% ethanol) and xylene. The stained chondrogenic cell pellets were mounted with DPX Mountant (Sigma-Aldrich) and analysed with the Mirax Desk digital slide scanner (Zeiss) using Mirax scan software.

2.15 Statistical analysis

GraphPad Prism version 6 was used for the statistical analyses of the data. The results were represented as mean ± standard error of the mean (SEM). Normality was tested by using D'Agostino and Pearson omnibus normality test. When data were normally distributed, an unpaired two-tailed Student T-test (2 groups) or one-way ANOVA (Tukey multiple comparison test of 3 or more groups) was performed. The nonparametric Mann-Whitney test (2 groups) or Kruskal-Wallis test (Dunn's post hoc comparison of 3 or more groups) was used for data which were not normally distributed. *$P < 0.05$, **$P < 0.01$, ***$P < 0.001$, ****$P < 0.0001$

3 Results

3.1 Morphology of DPSC isolated via the explant method

To unravel the neuroprotective and -regenerative properties of DPSC *in vitro*, a DPSC culture was established in our lab. DPSC were isolated by means of the explant methodology. After adherence of the dental pulp explants to the culture plates, DPSC start to grow out of the tissue and adhere to the plastic surface (Fig 4A, B). Approximately 10-14 days after dental pulp isolation, DPSC reach 70-80% confluency. The morphology of the cultured DPSC resembles that of fibroblast-like cells, varying from a spindle-like shaped to a polygonal shaped appearance, thereby forming a heterogeneous cell culture (Fig 4C).

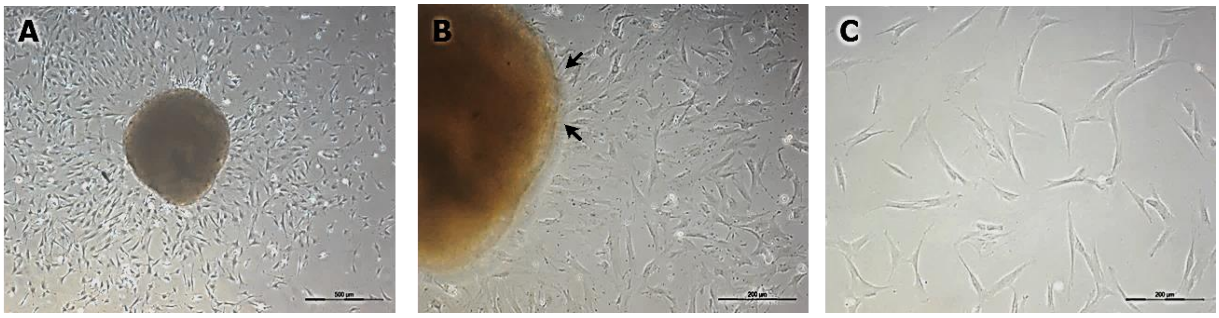

Figure 4: Morphologic characterization of DPSC isolated by the explant methodology. (A, B) DPSC migrate out of the dental pulp explants and show adherence to plastic surface. **(B)** At higher magnification, outgrowth of DPSC from the explant is visualized (arrows). **(C)** After the isolation procedure, a heterogeneous DPSC culture is established, in which cellular morphology ranges from spindle-like shaped to polygonal shaped. Scale bar A: 500 µm and B,C: 200 µm.

3.2 Comparison of the trilineage differentiation potential of DPSC and HDF

DPSC and fibroblasts are known to share many phenotypical characteristics, such as surface expression markers and morphology. Therefore, HDF are included as control cells for DPSC in this study. Due to their similarities, it is important to define differences in functional properties between these two cell types. Because the stem cell characteristics, biology and multilineage differentiation capacity of DPSC have been characterized extensively, we explored whether HDF possess potential stem cell-like features. For this purpose, the trilineage differentiation potential of DPSC and HDF into osteoblast, adipoblasts and chondroblasts was compared. In addition, BM-MSC were included as positive controls.

3.2.1 Osteogenic differentiation

Induction of osteogenic differentiation results in strong uniform ALP expression in differentiated DPSC (Fig 5A-C) and BM-MSC (Fig 5E) cultures in comparison with undifferentiated control cells (Fig 5F-H, J). In contrast, ALP expression could not be observed in HDF (Fig 5D). To demonstrate the formation of calcified nodules, osteogenically differentiated cells were stained with Alizarin Red S. Scarce calcium deposits (orange stain) are detected in osteogenically differentiated DPSC (Fig 5K-M), while calcified nodules are completely absent in osteogenic-induced HDF and BM-MSC (Fig 5N, O). Undifferentiated control cultures display no calcified deposits (Fig 5P-T).

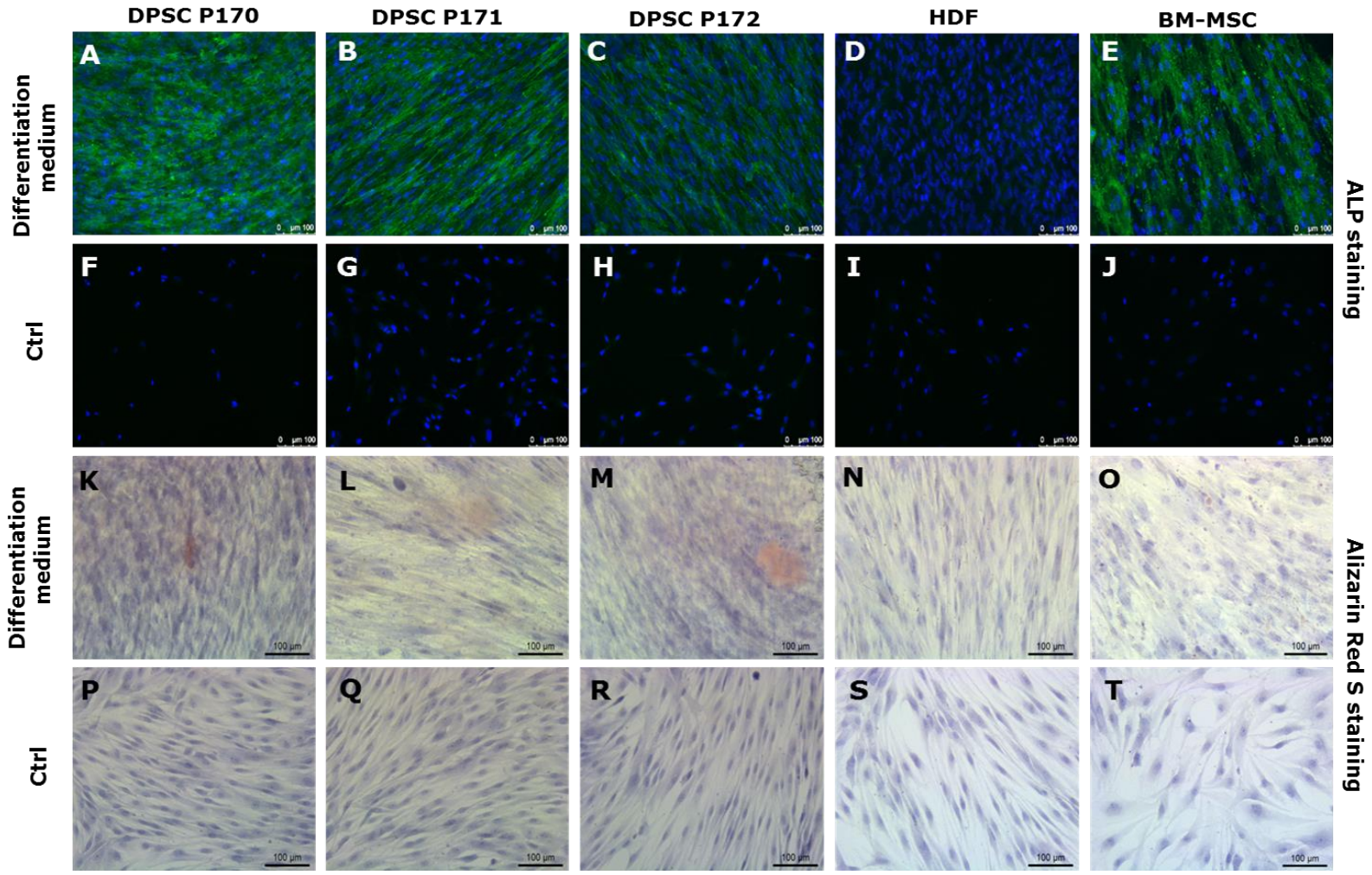

Figure 5: Osteogenic differentiation of DPSC, HDF and BM-MSC. (A-E) ALP expression is induced in osteogenically differentiated DPSC (A-C) and BM-MSC (E). No ALP reactivity is observed in osteogenically differentiated HDF (D). **(F-J)** Undifferentiated control cells display no ALP expression. **(K-O)** Alizarin Red S staining demonstrates singular calcium deposits in osteogenic-induced DPSC (K-M), while no calcium nodules are present in osteogenically differentiated HDF and BM-MSC (N, O). **(P-T)** No calcium deposits are detected in undifferentiated control cultures. Scale bar A-T: 100 µm; ALP: alkaline phosphatase

3.2.2 Adipogenic differentiation

After 21 days on adipogenic differentiation medium, transparent lipid droplets are visualized in the cell cytoplasm via the phase-contrast microscope. Immunocytochemical analysis revealed that adipogenic differentiation of HDF and BM-MSC (Fig 6D, E) results in *de novo* expression of FABP-4 in a subset of cells compared to undifferentiated control cells (Fig 6I, J). In contrast, DPSC display no pronounced FABP-4 immuno-reactivity (Fig 6A-C). To assess functional characteristics of the adipogenically differentiated cells, lipid-containing vacuoles were stained with ORO. In accordance with the FABP-4 staining, only subsets of HDF and BM-MSC demonstrate large intracellular lipid vacuoles (Fig 6N, O). Moreover, in adipogenic-induced DPSC cultures, small intracellular lipid droplets are observed, which are homogenously distributed within the whole cell population (Fig 6K-M). However, no ORO^+ lipid droplets are shown in undifferentiated cell cultures (Fig 6P-T).

3.2.3 Chondrogenic differentiation

Chondrogenic differentiation was induced using a 3D cell pellet culture. Following 3 weeks on differentiation medium, cellular spheres are formed, consisting of a cell population embedded in extracellular matrix. To demonstrate the production of glycosaminoglycans and glycoproteins, an Alcian blue staining was performed. Chondrogenically differentiated DPSC (Fig 7A-C) and BM-MSC pellets (Fig 7E) show abundant production of glycosaminoglycans and glycoproteins (blue stain). Generally, BM-MSC pellets display a more structured pattern of extracellular matrix than DPSC pellets. In contrast, low levels of glycosaminoglycans and glycoproteins are detected in chondrogenically differentiated HDF pellets (Fig 7D). Furthermore, minimal extracellular matrix is formed in undifferentiated control cell pellets (Fig 7F-H). Additionally, cellular pellets were immunohistochemically analysed for aggrecan expression, which is a critical component of cartilage. Differentiated BM-MSC (Fig 7M) demonstrate strong aggrecan immune-reactivity, while relative low expression is observed in chondrogenic-induced HDF (Fig 7L). However, no aggrecan expression is shown in chondrogenically differentiated DPSC (Fig 7I-K).

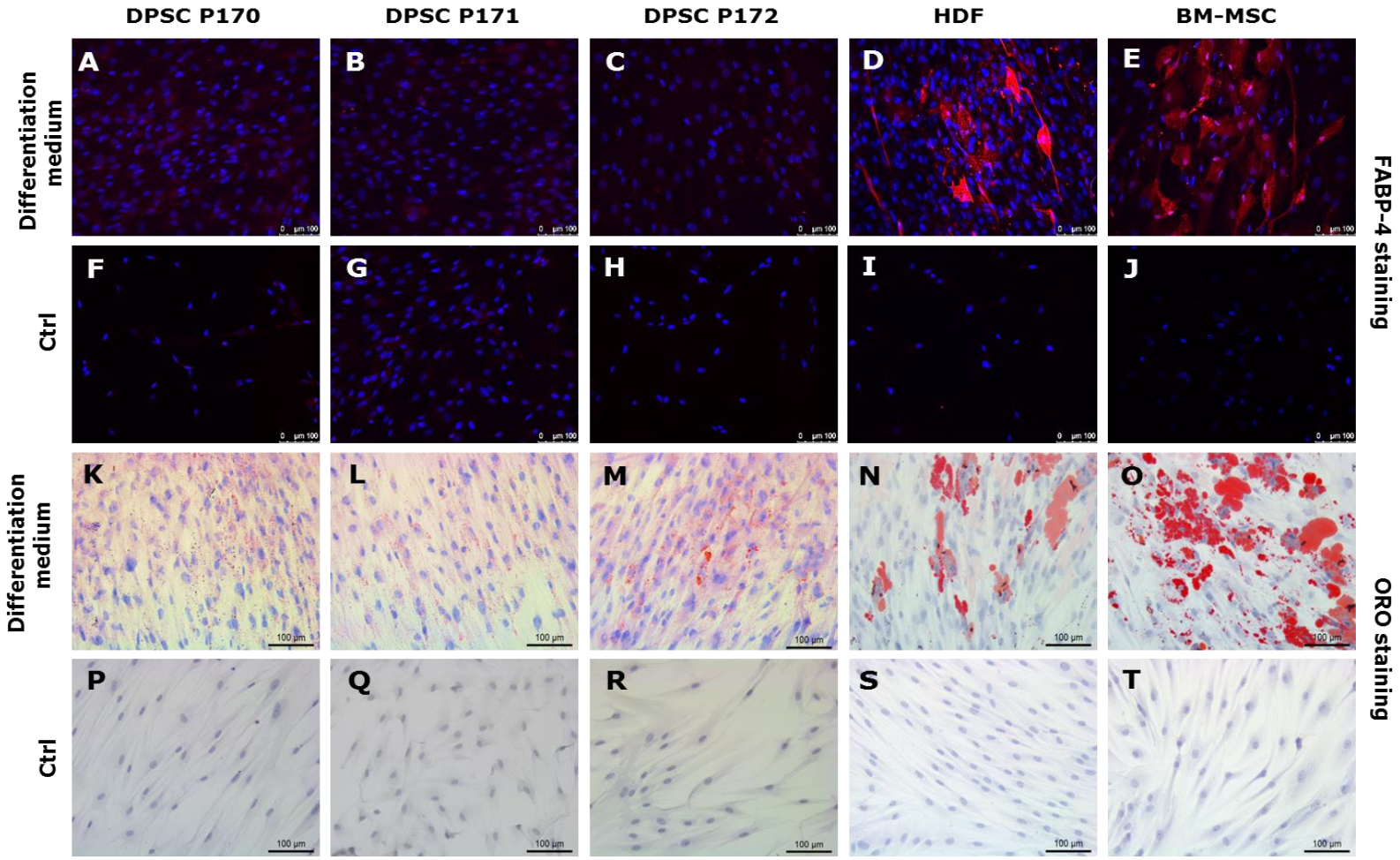

Figure 6: Adipogenic differentiation of DPSC, HDF and BM-MSC. (A-E) Adipogenically differentiated DPSC (A-C) show no pronounced FABP-4 immune-reactivity. In contrast, adipogenic-induced HDF and BM-MSC (D, E) display marked FABP-4 expression. **(F-J)** No FABP-4 reactivity is observed in undifferentiated control cells. **(K-O)** Lipid droplets of adipogenically differentiated cells were demonstrated via ORO staining. Adipogenic-induced DPSC (K-M) display small, homogenous distributed lipid droplets. Large lipid vacuoles are visualized in adipogenically differentiated HDF and BM-MSC (N, O). **(P-T)** Lipid droplets are absent in undifferentiated DPSC, HDF and BM-MSC. Scale bar A-T: 100 µm; FABP-4: fatty acid binding protein 4; ORO: Oil Red O

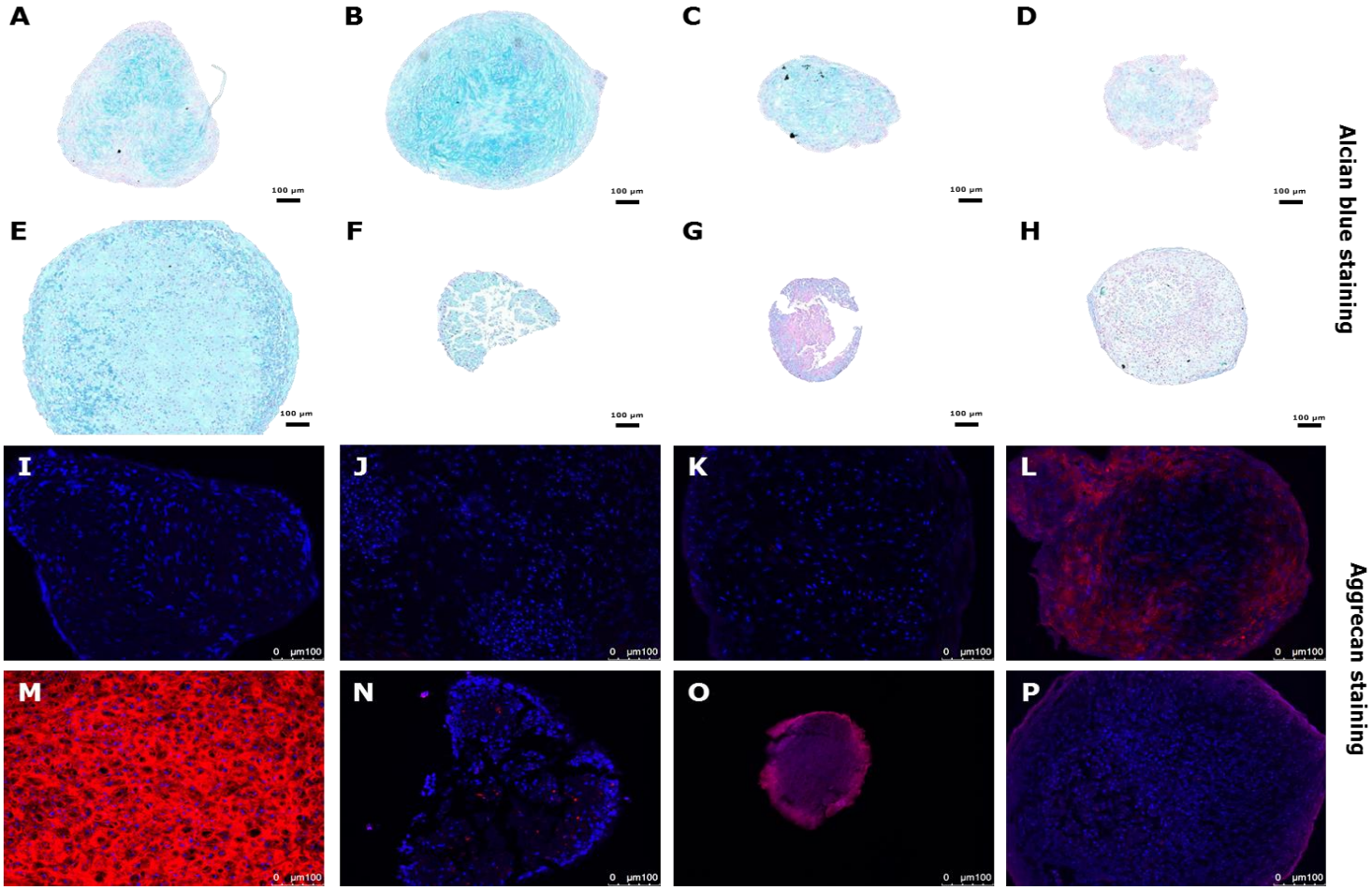

Figure 7: Chondrogenic differentiation of DPSC, HDF and BM-MSC. (A-H) Alcian Blue staining performed on chondrogenically differentiated (A-E) and control cell pellets (F-H). Chondrogenic cell pellets of DPSC (A-C) and BM-MSC (E) demonstrate abundant production of glycosaminoglycans and glycoproteins. However, the extracellular matrix show a more structured pattern in chondrogenically differentiated BM-MSC (E) than in chondrogenic-induced DPSC (A-C). Relative low levels of extracellular matrix proteins are detected in chondrogenic HDF pellets (D). Control pellets of BM-MSC (F), DPSC (G) and HDF (H) display minimal extracellular matrix formation. **(I-P)** Aggrecan staining performed on chondrogenically differentiated (I-M) and control cell pellets (N-O). Chondrogenically differentiated DPSC (I-K) display no aggrecan immune-reactivity, while chondrogenic-induced BM-MSC (M) express high levels of aggrecan. Chondrogenically differentiated HDF (L) are weakly immune-reactive for aggrecan. BM-MSC, DPSC and HDF control pellets (respectively N, O and P) demonstrate no aggrecan expression. Scale bar A-P: 100 µm

3.3 Neuroprotective effects of DPSC *in vitro*

Conferring neuroprotection via providing neurotrophic support represents an important mechanism of DPSC-based cell therapy in ischaemic stroke. It has been described that the secretome of DPSC consists of a variety of growth factors, including several neurotrophic factors [35, 36]. To identify secreted neurotrophic factors by DPSC, a human growth factor array on CM-DPSC was previously performed in our lab. A wide variety of growth factors were detected in CM-DPSC, of which 17 growth factors were identified with known neurotrophic effects (Fig 8). As shown in the graph, insulin-like growth factor binding protein 6 (IGFBP-6) and IGF-II are most abundantly secreted by DPSC.

Since the presence of multiple neurotrophic factors was demonstrated in CM-DPSC, the ability of DPSC to confer neuroprotection to ischaemic neuronal cells was evaluated. For this purpose, an OGD neuronal survival assay was developed. In this assay, pCN were exposed to 0.3% O_2 and glucose-free medium for 3 h or 6 h. Subsequently, pCN were cultured under reperfusion conditions (2.3% O_2) for 24 h. The aim of this assay is to assess neuronal survival of ischaemic pCN in response to CM-DPSC exposure. In addition, the neuroprotective effects of several paracrine factors were evaluated to identify key paracrine factor(s) responsible for neuronal survival. Prior to employ the OGD assay for neuroprotection studies, the pCN surface coating for the OGD assay was optimized, since pCN cultures are known to be very sensitive to mechanical stress. Furthermore, an initial evaluation of the neuroprotective capacity of multiple growth factors, CM-DPSC, CM-HDF and CM-BM-MSC in the OGD survival assay was performed to gain insight into the optimal read-out and treatment protocol for this assay.

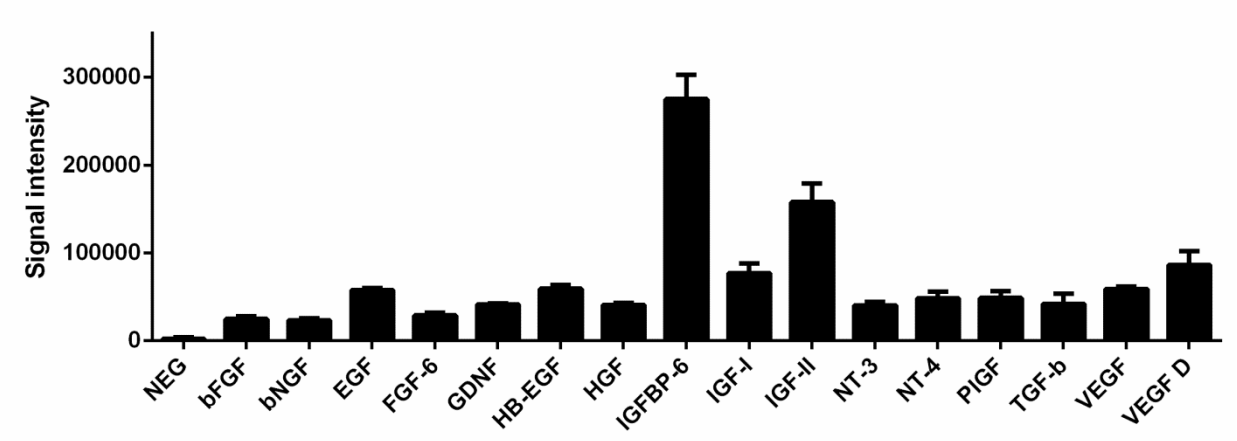

Figure 8: Overview of neurotrophic factors present in CM of DPSC. Based on a growth factor array performed on CM of DPSC, 17 neurotrophic factors were identified. IGFBP-6 and IGF-II are shown to be most abundantly present in CM of DPSC. This array was performed on CM of DPSC from 3 different donors. Data are represented as mean ± SEM. Data were obtained by Y. Dillen.

3.3.1 Optimization of pCN surface coating in the OGD assay

Exploring the ideal surface coating for pCN is critical to obtain optimal results in the OGD assay, since pCN cultures are known to be susceptible to mechanical forces and easily detach from culture plates. Furthermore, coating of the culture plate surfaces is essential to support optimal maturation of neuronal cells *in vitro*. In order to screen for the optimal surface coating for the OGD assay, pCN were cultured for 5 days on multiple surface coatings. Used surface coatings included poly-D-lysine (PDL), poly-L-ornithine (PLO), fibronectin (Fibr) and laminin (Lam). Double coatings of PDL/PLO with fibronectin or laminin were also included. For each surface coating, two different concentrations were tested (table 2). After the maturation period of 5 days, baseline cell viability was assessed by means of PI staining (T0). Subsequently, an OGD assay was performed to obtain information on pCN attachment to the different surface coatings after mechanical handling. For this purpose, pCN were exposed for 5 h to OGD and cell viability was measured immediately after (T1) and 24 h (T2) after OGD.

Table 2: Overview of the used concentrations for the different pCN surface coatings.

Surface Coating	Concentration (1)	Concentration (2)	Supplier
Poly-D-lysine (PDL)	50 µg/ml	100 µg/ml	R&D Systems
Poly-L-ornithine (PLO)	50 µg/ml	100 µg/ml	Sigma-Aldrich
Fibronectin (Fibr)	5 µg/m	10 µg/ml	R&D Systems
Laminin (Lam)	5 µg/ml	10 µg/ml	Merck Millipore
PDL-Lam	50 µg/ml - 2 µg/ml	50 µg/ml - 5 µg/ml	
PDL-Fibr	50 µg/ml - 2 µg/ml	50 µg/ml - 5 µg/ml	
PLO-Lam	50 µg/ml - 2 µg/ml	50 µg/ml - 5 µg/ml	
PLO-Fibr	50 µg/ml - 2 µg/ml	50 µg/ml - 5 µg/ml	

Merck Millipore: Overijse, Belgium

Seeding pCN on PDL (Fig 9A, E), Lam (Fig 9C, G), Fibr (Fig 9D, H) and PDL-Lam (Fig 9I, M) surface coatings results in the formation of dense cellular aggregates from which small neurites extend. Occasionally, connections are observed between adjacent aggregates. When culturing pCN on PDL-Fibr (Fig 9J, N) and PLO-Lam (Fig 9K, O) surface coatings, large neuronal aggregates are formed which are strongly interconnected with each other. Additionally, pCN cultured on PLO (Fig 9B, F) and PLO-Fibr (Fig 9L, P) coated culture plate surfaces display characteristics of a mature, heterogeneous neuronal network with multiple strong interconnections. To assess the optimal surface coating for pCN attachment, an OGD experiment was performed as described above. Neuronal cells cultured on 100 µg/ml PLO coating and PLO-Fibr coating (50 µg/ml – 2 µg/ml and 50 µg/ml - 5 µg/ml) demonstrate the highest cell viability/attachment after 5 h (T1) on OGD conditions (respectively 101 ± 19.6% ; 78 ± 1.6% and 95 ± 17.7%) (Fig 9Q, R). Furthermore, 24 h after OGD (T2), pCN seeded on 100 µg/ml PLO and PLO-Fibr surface coatings still display 26 ± 5.7 %, 24 ± 1% and 29 ± 4.3% neuronal survival (Fig 9Q, R). Based on the results of the OGD experiment and the observed neuronal culture morphology, 100 µg/ml PLO seems to be the optimal surface coating for pCN in OGD experiments, since relative high pCN attachment could be established. Therefore, this surface coating is further employed in each OGD experiment throughout this study.

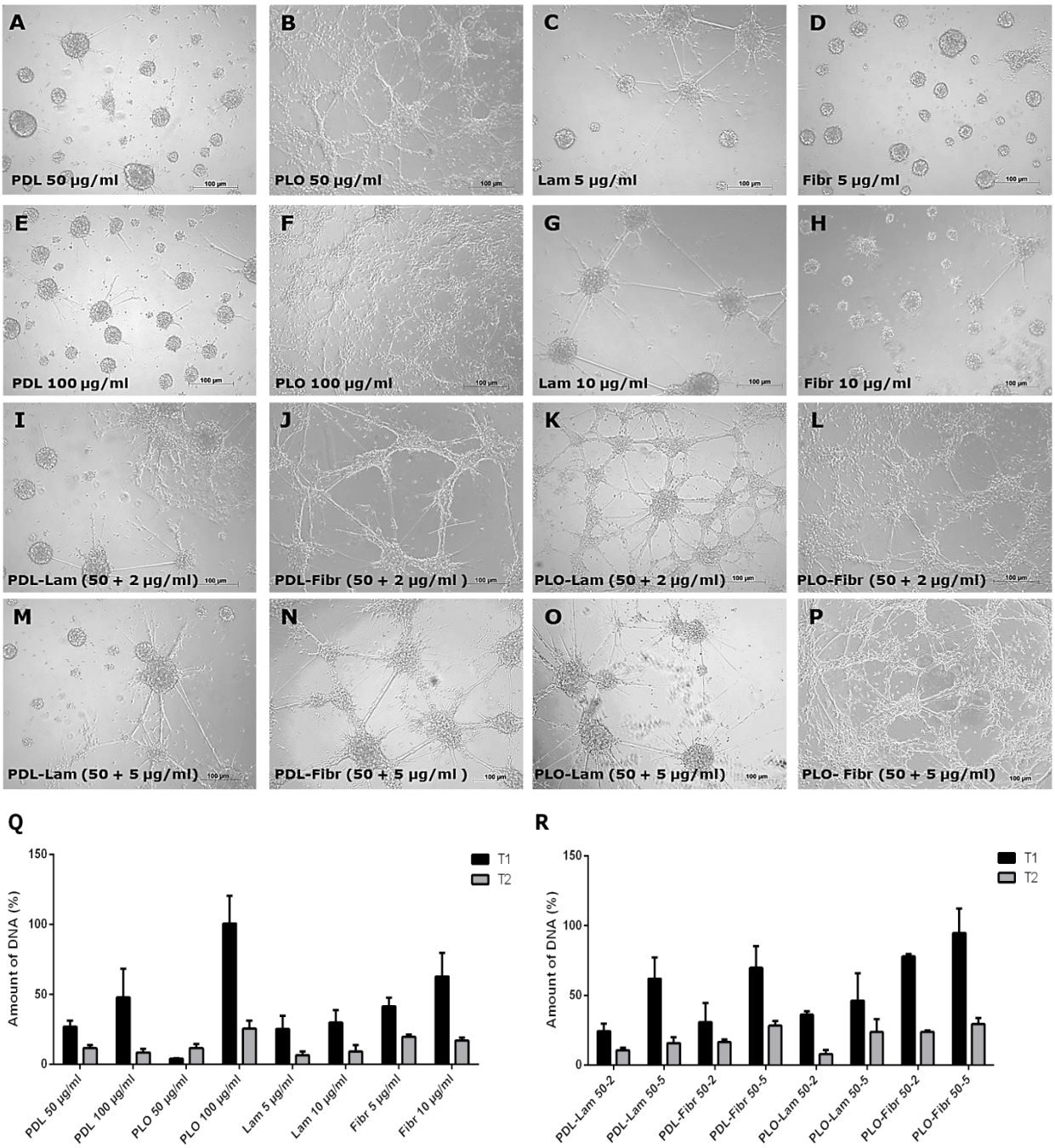

Figure 9: Morphology and viability analysis of pCN cultured on multiple surface coatings. (A-P) Phase-contrast images of pCN cultured on different surface coatings. Cells were seeded at a density of 2.4 x 10^5 cells/cm^2. Neuronal cells cultured on PLO (B, F) or PLO-Fibr (L, P) double coating form a mature neuronal network, with multiple strong connections. Culturing of pCN on other surface coatings results in the formation of neuronal aggregates which are (occasionally) interconnected with each other. Scale bar A-P: 100 µm **(Q-R)** pCN were exposed to OGD conditions for 5 h, after which neuronal viability was assessed immediately after (T1) and 24 h after (T2) OGD with PI staining. Data were normalized to the baseline neuronal survival values (T0). PLO (100 µg/ml) (Q), PLO-Fibr (50 - 2 µg/ml) and PLO-Fibr (50 – 5 µg/ml) (R) demonstrate the highest pCN attachment after 5 h on OGD (T1). Data are represented as mean ± SEM (three technical replicates). PDL: Poly-D-lysine; PLO: Poly-L-ornithine; Lam: Laminin; Fibr: Fibronectin; PDL-Lam: Poly-D-lysine-laminin; PDL-Fibr: Poly-D-lysine-fibronectin; PLO-Lam: Poly-L-ornithine-laminin; PLO-Fibr: Poly-L-ornithine-fibronectin.

3.3.2 Exploration of the OGD neuronal survival assay for neuroprotection studies

The neuroprotective effects of multiple paracrine factors and CM-DPSC, CM-HDF and CM-BM-MSC were evaluated by means of an OGD neuronal survival assay. However, in order to obtain reproducible results, it is important to screen for the optimal read-out and treatment protocol. Therefore, in this study, two different treatment protocols and viability read-outs were explored. The experimental setup of the used treatment protocols are depicted in figure 3. Neuronal cultures were subjected to OGD conditions for 3 h or 6 h. Prior to OGD exposure, baseline neuronal survival was assessed (T0) to which obtained fluorescence values were normalized. In the first (post-OGD) treatment protocol, CM and various concentrations of BDNF, GDNF and IGF-II, of which the neuroprotective effects have been previously described, were added to the pCN cultures immediately after OGD (Fig 3A). Neuronal viability, measured via PI staining with addition of lysis and stabilisation buffer, was used as read-out.

In the post-OGD treatment protocol, no improvement in neuronal survival is observed following addition of BDNF, GDNF and IGF-II at various concentrations after 3 h (500 ng/ml BDNF: 61 ± 1.1%; 50 ng/ml GDNF: 52 ± 3.7%; 500 ng/ml IGF-II: 60 ± 2.3%) and 6 h (500 ng/ml BDNF: 42 ± 6%; 50 ng/ml GDNF: 48 ± 3.2%; 500 ng/ml IGF-II: 32 ± 2.2%) of OGD compared to control (3 h OGD: 59 ± 1%; 6 h OGD: 50 ± 0.9%) (Fig 10A, B, C). In addition, CM of HDF, DPSC and BM-MSC do not provide any protection following 3 h (CM-HDF: 58 ± 3.2%; CM-DPSC: 48 ± 2.8%; CM-BM-MSC: 50 ± 2.4%; Ctrl: 59 ± 1%) and 6 h (CM-HDF: 35 ± 1.1%; CM-DPSC: 29 ± 2.1%; CM-BM-MSC: 36 ± 3.4%; Ctrl: 50 ± 0.9%) of OGD (Fig 10D).

Since no effect of CM and growth factors on neuronal survival could be observed post-OGD, it was investigated whether addition of CM and growth factors during OGD could prevent neuronal cell death (Fig 3B). Because of the impermeability of PI to viable cells, PI staining without addition of lysis and stabilisation buffer was used to measure neuronal death. All obtained fluorescence data were normalized to the baseline neuronal cell death values measured before the start of OGD (T0). In accordance with the previous treatment protocol, the various concentrations of BDNF, GDNF and IGF-II have no significant effect on neuronal survival following 3 h (500 ng/ml BDNF: 162 ± 9.2%; 50 ng/ml GDNF: 154 ± 2.1%; 500 ng/ml IGF-II: 166 ± 4.4%; Ctrl: 156 ± 2.4%) and 6 h (500 ng/ml BDNF: 256 ± 39.8%; 50 ng/ml GDNF: 233 ± 41%; 500 ng/ml IGF-II: 232 ± 29.8%; Ctrl: 284 ± 87.8%) of OGD (Fig 11A, B, C). Furthermore, CM-HDF and CM-DPSC are not able to reduce neuronal death after 3 h (CM-HDF: 158 ± 5.2%; CM-DPSC: 163 ± 3.6%; Ctrl: 162 ± 8.4%) and 6 h (CM-HDF: 197 ± 53.2%; CM-DPSC: 134 ± 6.2%; Ctrl: 199 ± 44.9%) of OGD (Fig 11D).

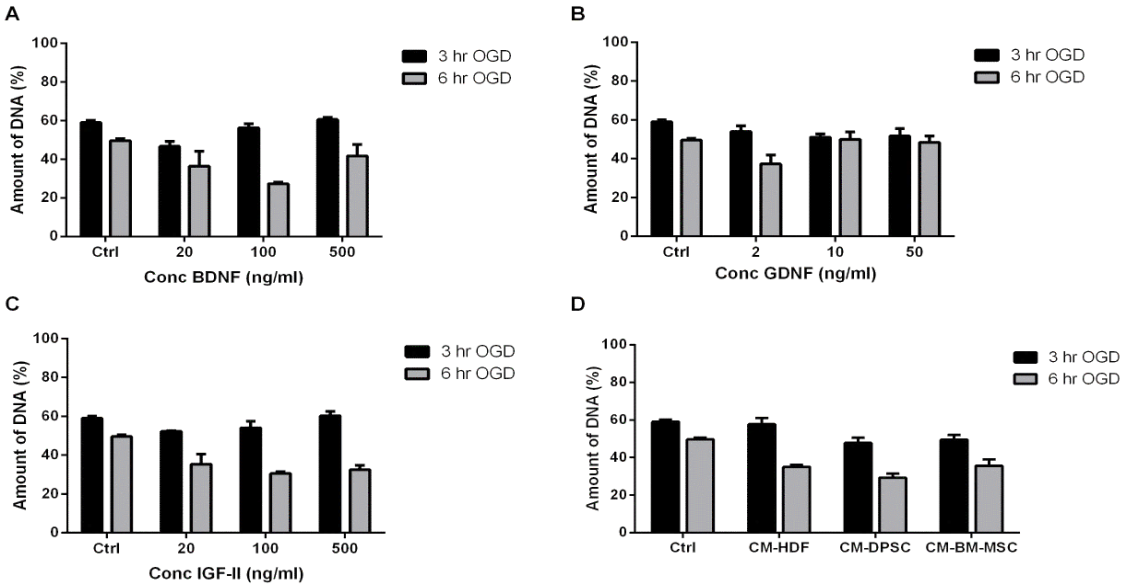

Figure 10: Post-OGD treatment effects of CM and growth factors. pCN were seeded at a density of 2.4 x 10^5 cells/cm^2. Neuronal cultures were cultured in OGD conditions for 3 h or 6 h. After OGD, pCN were exposed to CM of HDF, DPSC and BM-MSC or to various concentrations of BDNF, GDNF and IGF-II. PI staining (with lysis and stabilization buffers) was used to assess neuronal viability. Data were normalized to the baseline neuronal survival values (T0). Different concentrations of BDNF **(A)**, GDNF **(B)** and IGF-II **(C)** have no effect on neuronal survival after 3 h and 6 h OGD. In addition, CM of HDF, DPSC and BM-MSC **(D)** are unable to improve neuronal viability following 3 h and 6 h OGD. Data are represented as mean ± SEM (three technical replicates). A Kruskal-Wallis test (Dunn's post hoc comparison) was used for data analysis.

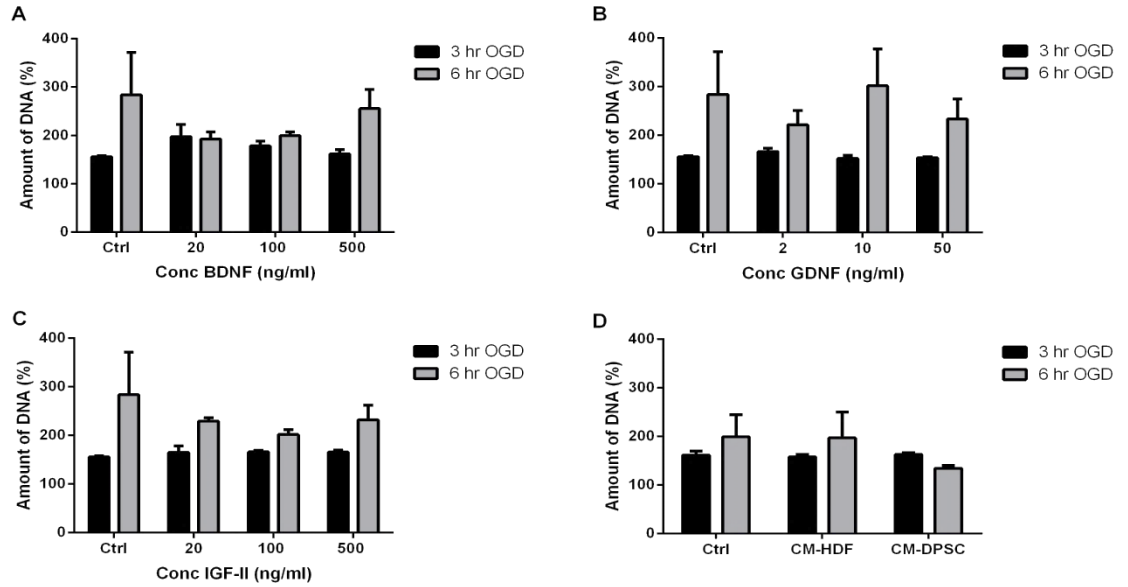

Figure 11: Effect of CM and growth factor incubation during OGD on pCN survival. pCN were seeded at a density of 2.4 x 10^5 cells/cm^2. Neuronal cultures were cultured in OGD conditions for 3 h or 6 h. During OGD, pCN were exposed to CM of HDF, DPSC and BM-MSC or to various concentrations of BDNF, GDNF and IGF-II. PI staining (without lysis and stabilization buffers) was used to assess neuronal death. Data were normalized to the baseline neuronal cell death values (T0). Different concentrations of BDNF **(A)**, GDNF **(B)** and IGF-II **(C)** are unable to reduce neuronal death following 3 h and 6 h OGD. Furthermore, CM-DPSC and CM-HDF have no effect on neuronal survival after 3 h and 6 h OGD **(D)**. Data are represented as mean ± SEM (three technical replicates). A Kruskal-Wallis test (Dunn's post hoc comparison) was used for data analysis.

3.4 Neuroregenerative effects of DPSC *in vitro*

The recruitment of NSC toward the stroke lesion is a crucial step in the endogenous regeneration of damaged neural tissue after cerebral ischaemia. To evaluate whether DPSC are able to promote this type of endogenous repair, the migration of NSC in response to CM of DPSC was assessed via a transwell migration assay. In addition, the migratory effect of several trophic factors on NSC was evaluated. This will provide information on which paracrine factor(s) could be responsible for the migratory effect of DPSC and could eventually be upregulated in DPSC via lentiviral transduction. Furthermore, it was investigated whether addition of the key paracrine factor responsible for NSC migration is able to enhance the migratory effect of DPSC.

3.4.1 CM of DPSC promotes the migration of NSC

To assess the neuroregenerative effects of DPSC, NSC were seeded at 5 x 10^4 cells per insert and were exposed for 24 h to CM-HDF, CM-DPSC P169, CM-DPSC P172 and CM-BM-MSC. SDF-1 diluted in α-MEM (100 ng/ml) was included as positive control. After 24 h, migrated cells were visualized via crystal violet staining. As displayed in figure 12A, CM-DPSC promotes the migration of NSC to a greater extent than the negative control (Fig 12A). Furthermore, CM-DPSC confers a superior migratory effect on NSC compared to CM-HDF (Fig 12A). Quantitative analysis confirmed that CM-DPSC (CM-DPSC P169: 19 ± 1.4%; CM-DPSC P172: 21 ± 1.6%) significantly increases the migration of NSC in comparison with control medium (6 ± 1.5%) and CM-HDF (8 ± 0.9%) (Fig 12B). Although not significant, CM-DPSC seems to have a higher migratory effect on NSC than CM-BM-MSC (13 ± 1.4%) and SDF-1 (16 ± 0.9%) (Fig 12B).

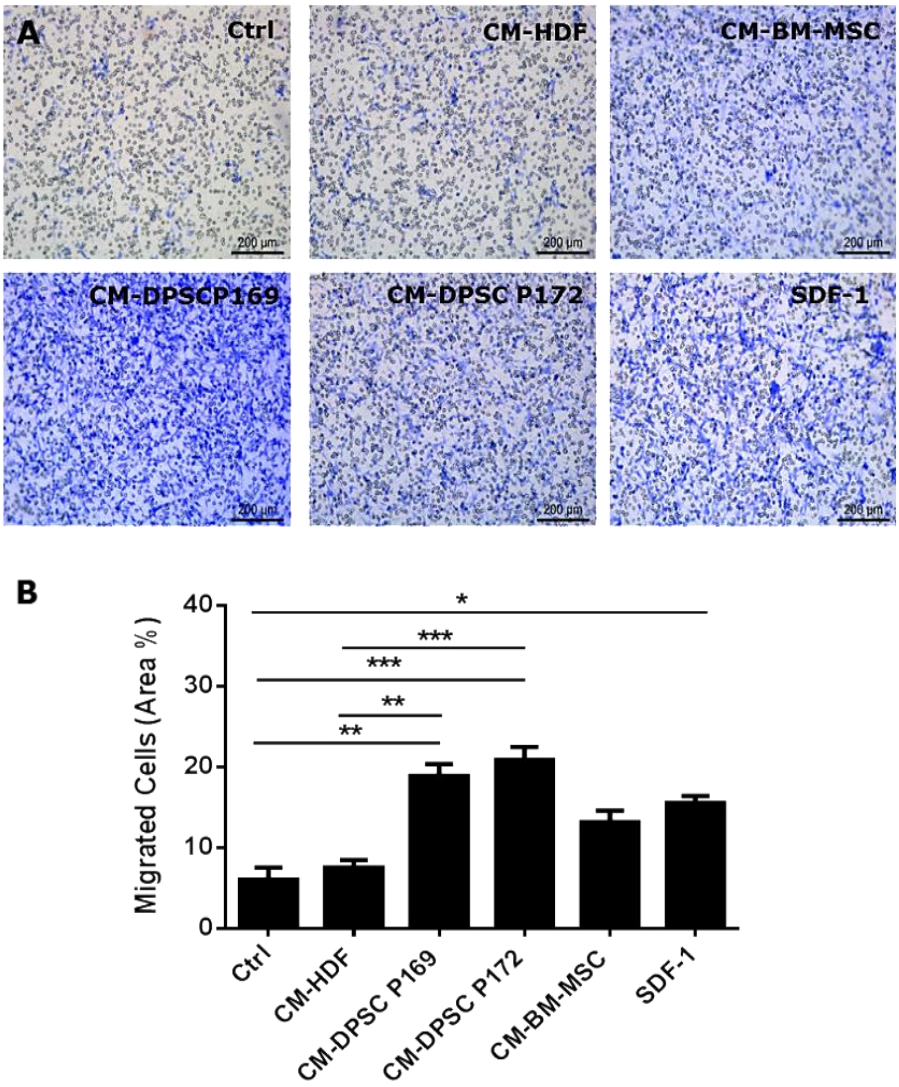

Figure 12: CM of DPSC has a significant migratory effect on NSC. Transwell inserts seeded with 5 x 10^4 NSC were incubated for 24 h with control medium, CM-HDF, CM-DPSC P169, CM-DPSC P172, CM-BM-MSC and SDF-1. SDF-1 was included as positive control. **(A)** Migrated NSC were visualized by crystal violet staining. Scale bar: 200 µm **(B)** Quantification of the migrated cells per condition. CM-DPSC significantly enhances NSC migration compared to CM-HDF and control medium. Data are represented as mean ± SEM (n=8). A Kruskal-Wallis test (Dunn's post hoc comparison) was used for data analysis. *P < 0.05, **P < 0.01, ***P < 0.001

3.4.2 Migratory effect of neurotrophic factors on NSC

In order to get an indication of which paracrine factors are responsible for the migratory effect of DPSC, NSC migration was evaluated in response to several growth factors (BDNF, GDNF, NGF, NT-3 and IGF-II). Transwell inserts were seeded with 5 x 10^4 NSC and were incubated for 24 h with 100 ng/ml BDNF, GDNF, NGF, IGF-II and NT-3 (diluted in α-MEM). 100 ng/ml SDF-1 was included as positive control. Crystal violet staining demonstrated that IGF-II, NT-3 and SDF-1 exert a greater migratory capacity than control medium, BDNF, GDNF and NGF (Fig 13A). Furthermore, quantitative analysis showed that NSC migration is significantly enhanced by IGF-II (12 ± 1.1%) and SDF-1 (15 ± 1.0%) compared to control (4 ± 1.0%) (Fig 13B). In contrast, NSC migration is not significantly increased by BDNF (9 ± 1.4%), GDNF (8 ± 1.1%), NGF (8 ± 1.6%) and NT-3 (8 ± 0.8%) in comparison with control medium (Fig 13B). Based on their migratory effect, IGF-II and SDF-1 represent interesting key paracrine factors which could possibly be accountable for DPSC-mediated NSC migration.

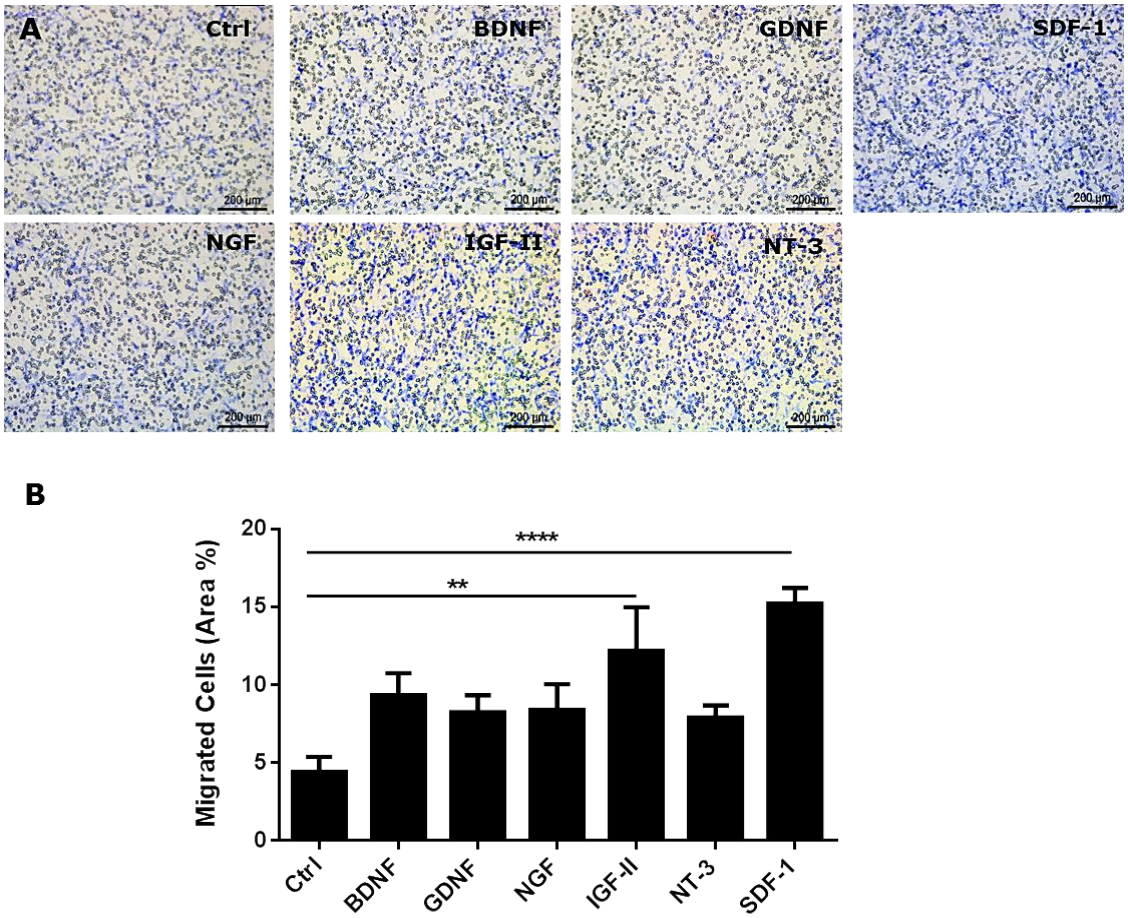

Figure 13: IGF-II and SDF-1 significantly promote NSC migration. NSC were seeded at 5 x 10^4 cells per insert and were incubated for 24 h with control medium, BDNF, GDNF, NGF, IGF-II, NT-3 and SDF-1. All growth factors were diluted in α-MEM at a final concentration of 100 ng/ml. SDF-1 was included as positive control. **(A)** Migrated NSC were visualized by crystal violet staining. Scale bar: 200 µm **(B)** Quantification of the migrated cells per condition. IGF-II and SDF-1 have a significant higher migratory effect on NSC compared to control medium. Data are represented as mean ± SEM (n=7). A Kruskal-Wallis test (Dunn's post hoc comparison) was used for data analysis. **P < 0.01, ****P < 0.0001

3.4.3 IGF-II addition does not further increase the migratory effect of CM-DPSC

Because of its migratory effect on NSC, IGF-II represents an attractive candidate to stimulate the neuroregenerative effects of DPSC via lentiviral transduction in future experiments. As a first step, we investigated whether addition of IGF-II to CM-DPSC could enhance the migratory effect of DPSC on NSC. Therefore, NSC seeded in transwell inserts were exposed to control medium, CM-DPSC P169 and CM-DPSC P172 with or without addition of 100 ng/ml IGF-II. SDF-1 diluted in α-MEM (100 ng/ml) was used as a positive control. Crystal violet staining demonstrates no additional effect of IGF-II on DPSC-mediated NSC migration (Fig 14A). These findings were endorsed by quantitative analysis of the stainings, which showed that addition of IGF-II does not enhance the migratory effect of DPSC on NSC (CM-DPSC P169: 17 ± 3.6% vs CM-DPSC P169 + IGF-II: 17 ± 3.9%; CM-DPSC P172: 17 ± 0.2% vs CM-DPSC P172 + IGF-II: 13 ± 0.1%) (Fig 14B).

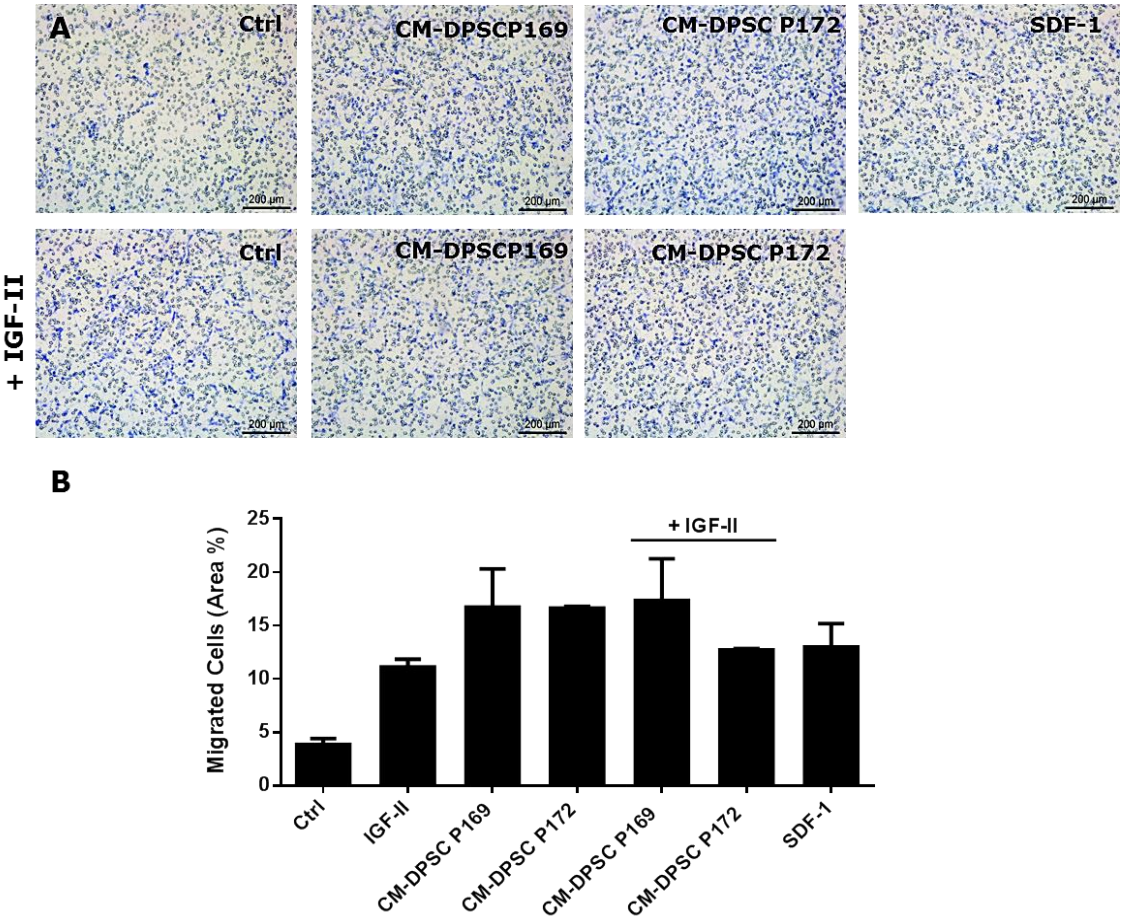

Figure 14: IGF-II addition to CM-DPSC does not enhance DPSC-mediated NSC migration. Transwell inserts were seeded with 5 x 10^4 NSC and were incubated for 24 h with control medium, CM-DPSC P169 and CM-DPSC P172 (with or without addition of 100 ng/ml IGF-II). 100 ng/ml SDF-1 diluted in α-MEM was included as positive control. **(A)** Migrated NSC were visualized by crystal violet staining. Scale bar: 200 µm **(B)** Quantification of the migrated cells per condition. Supplementation of IGF-II to CM-DPSC has no additional effect on the migratory effect of DPSC. Data are represented as mean ± SEM (n=2). A Kruskal-Wallis test (Dunn's post hoc comparison) was used for data analysis.

4 Discussion

Since the current treatment strategies for ischaemic stroke often fail to improve the functional outcome of patients, cell-based therapies are extensively explored within the field of stroke research. The stem cells' ability to protect penumbral neuronal cells from apoptosis and to stimulate endogenous repair mechanisms hold great clinical promise for cell-based therapies as stroke treatment. Because of their neurogenic properties, DPSC represent promising candidates for this purpose [45, 58, 60, 61]. However, in order to use DPSC as cell-based therapy in stroke, their potential beneficial mechanisms of action have to be characterized. In this study, the neuroprotective and neuroregenerative effects of DPSC were explored *in vitro* and compared with HDF and BM-MSC. First, the trilineage differentiation capacity of DPSC, HDF and BM-MSC was compared. Subsequently, the neuroprotective effects of DPSC were evaluated via an OGD neuronal survival assay. In this assay, the optimal surface coating for pCN cultures, different treatment protocols and neuronal survival read-outs were examined. Moreover, the neuroregenerative capacity of DPSC was investigated by assessing the effect of CM-DPSC on NSC migration via a transwell migration assay. In addition, the migratory effect of multiple neurotrophic factors was evaluated to identify key paracrine factor(s) responsible for NSC migration.

In order to determine whether DPSC confer neuroprotection and possess neuroregenerative effects *in vitro*, it is crucial to compare their neurorestorative effects with a control cell type. Since DPSC and fibroblasts share many characteristics, surface markers and possess the same morphology, HDF were included as control cells in this study. Because of their phenotypical similarities, it is important to distinguish DPSC and HDF based on functional properties, such as their differentiation capacity. Therefore, the trilineage differentiation potential of DPSC and HDF into osteoblasts, adipoblasts and chondroblasts was compared. BM-MSC were included as positive control, since their trilineage differentiation capacity has been extensively studied [62]. In the present study, we showed that osteogenic differentiation induced ALP expression in BM-MSC and DPSC, but not in HDF. However, the scarcity of calcium deposits demonstrated by Alizarin Red S staining, indicates that complete osteogenic differentiation was not yet established in DPSC and BM-MSC. Nevertheless, the observed ALP-immunoreactivity of osteogenically differentiated DPSC and BM-MSC suggests that an immature osteogenic phenotype was induced. Interestingly, adipogenic differentiation of HDF and BM-MSC had a comparable outcome in both cell types. Adipogenically differentiated HDF and BM-MSC were both characterized with FABP-4 expression and the presence of intracellular lipid vacuoles which indicate complete adipogenic differentiation. In contrast, differentiated DPSC displayed relative small intracellular lipid droplets, but demonstrated no FABP-4 expression which suggest that DPSC possess a lower adipogenic differentiation capacity compared to BM-MSC and HDF. In addition, subjecting BM-MSC to chondrogenic differentiation resulted in the production of extracellular matrix proteins and the expression of aggrecan, which is distinctive for chondroblasts. However, chondrogenic differentiation of DPSC was only partially accomplished, since DPSC demonstrated no aggrecan immunoreactivity. Furthermore, only weak chondrogenic differentiation was observed in differentiated HDF since low aggrecan immune-

reactivity and minimal glycosaminoglycan/glycoprotein production was detected in chondrogenic HDF pellets.

Gronthos et al. were one of the first to explore the multilineage differentiation potential of DPSC. Their group demonstrated the osteogenic, odontogenic, adipogenic and neurogenic differentiation capacity of DPSC [22, 24]. Afterwards, this multilineage differentiation potential of DPSC was confirmed by multiple research groups [28, 63, 64]. However, several studies observed a relative low success rate of adipogenic differentiation in DPSC cultures [22, 28, 63]. Corresponding to our findings, it has been demonstrated that DPSC display a lower adipogenic differentiation capacity in comparison with BM-MSC and umbilical cord-derived MSC [22, 63]. In addition, we observed that HDF showed a greater adipogenic differentiation potential than DPSC. HDF used in this study were purchased from Sigma-Aldrich and were derived from human dermis. Recent studies reported that various progenitor cells reside within the dermis of the skin [65, 66]. It has been proposed that human dermal skin-derived fibroblasts are such skin progenitor cells and several studies explored their differentiation potential into mesodermal lineages. These studies have confirmed the multilineage differentiation capacity of HDF, which could possibly explain the adipogenic and weak chondrogenic differentiation of HDF in the present study [67, 68]. Furthermore, differences observed in the adipogenic and osteogenic differentiation between DPSC and HDF could be related to their environmental predisposition. HDF have been exposed to soft tissue development, which presumably favour adipogenic differentiation. On the other hand, DPSC are located within the hard tissue environment of the tooth, which could explain their greater osteogenic differentiation potential.

In general, complete differentiation of DPSC into adipoblasts and chondroblasts could not be established with the current differentiation kits. To further optimize the adipogenic and chondrogenic differentiation, other differentiation protocols could be used. For example, Struys et al. and Hilkens et al. obtained robust chondrogenic differentiation by culturing DPSC in D-MEM/F12 basal medium supplemented with insulin transferrin selenite, dexamethasone, ascorbate-phosphate, proline, pyruvate and transforming growth factor-β3 [28, 63]. Furthermore, adipogenic differentiation of DPSC could be induced by adding a 4-component cocktail, consisting of isobutyl-methylxanthine, dexamethasone, insulin and indomethacin, to α-MEM culture medium [64, 69]. Moreover, addition of peroxisome proliferator-activated receptor gamma (PPARγ) agonists such as rosiglitazone to the 4-component adipogenic induction medium are currently used to enhance the adipogenic differentiation process [69]. However, it must be noted that differences observed in DPSC differentiation could be related to patient variability. Therefore, new differentiation protocols should always be tested on DPSC derived from multiple patients.

Conferring neuroprotection to ischaemic neuronal cells represent an important mechanism of cell-based therapies in improving stoke outcome. Previous studies have demonstrated the neuroprotective capacity of DPSC in various models for neurodegenerative diseases. For example, in models for Parkinson's and Alzheimer's disease, co-culture of DPSC with dopaminergic and hippocampal neurons improved neuronal viability after exposure to disease-related neurotoxins [35, 59]. Furthermore, it has been shown that DPSC transplantation rescued motor neurons and

retinal ganglion cells in *in vivo* models for spinal cord injury and optical nerve injury [36, 70]. The neuroprotective capacity of DPSC in these studies was ascribed to neurotrophic factors secreted by the stem cells. DPSC are known to secrete a wide variety of neurotrophic factors including BDNF, GDNF, NGF and NT-3 [35, 36]. Inhibition of the neurotrophic tyrosine kinase receptors or the growth factors itself in the co-cultures resulted in attenuated neuroprotective effects of DPSC [35, 55]. In this study, the neuroprotective effects of DPSC in ischaemic stroke are of interest. Based on the promising results achieved by DPSC transplantation in stroke mouse models [45, 60, 61], we suggested that paracrine-mediated neuroprotection could be a possible mechanism of DPSC in neuronal repair. To evaluate the neuroprotective capacity of DPSC in an *in vitro* model for stroke, an OGD neuronal assay was performed, which is a commonly used assay to mimic ischaemic conditions *in vitro*.

Prior to employ the OGD neuronal survival assay for neuroprotection studies, the pCN surface coating was optimized. For *in vitro* neuronal cultures, coating of the culture plate surfaces is of great importance for the viability, maturation and purity of the culture. Moreover, the surface coating is crucial to increase neuronal adhesion, since pCN are very sensitive to mechanical stress [71, 72]. Commonly used coatings include ECM components, such as laminin and fibronectin, and polymeric amines (e.g. polyornithine and polylysine) [71]. In this study, we screened for the optimal surface coating by comparing the neuronal morphology and cellular viability of pCN cultured on multiple surface coatings. Neuronal cells cultured on PLO and PLO-Fibr coated culture plates demonstrated the highest cellular viability after OGD and had morphological characteristics of a mature neuronal network. PLO 100 µg/ml was the preferred pCN surface coating, since PLO-Fibr double coating is relative expensive and the coating process takes 1-2 days. In contrast to our findings, Ahlemeyer et al. showed reduced neuronal survival in hippocampal, cerebellar and cortical neuronal cells cultured on PLO compared to neuronal cultures seeded on poly-L-lysine [73]. However, in this report, neuronal cells were cultured in petri dishes coated with 10 µg/ml PLO whereas in our study, pCN were seeded in high attachment culture plates coated with 100 µg/ml PLO.

Since OGD is an important pathological hallmark during ischaemia, the OGD neuronal survival assay is a promising assay to investigate the neuroprotective capacity of DPSC in stroke. To evaluate paracrine-mediated neuroprotective effects by DPSC, pCN cultures were exposed to OGD conditions and were incubated with CM-DPSC, CM-HDF or CM-BM-MSC during or after OGD. In the present study, we were unable to observe any neuroprotective effects of CM-DPSC, CM-HDF and CM-BM-MSC on ischaemic neuronal cells. These findings are in conflict with the study of Song et al., which reported the neuroprotective capacity of DPSC on ischaemic astrocytes. Their group demonstrated that pre- and posttreatment of DPSC or CM-DPSC protected human astrocytes against OGD-induced cell death [56]. In accordance, pre- and posttreatment of OGD-exposed neurons with CM-BM-MSC resulted in increased neuronal survival [74, 75]. It must be noted that the majority of these studies use metabolic activity as read-out for neuronal viability. Since apoptotic cells are known to increase their metabolic activity in an attempt to survive, metabolic read-outs to evaluate neuronal survival is far from ideal and could generate misleading information. In contrast to the previous findings, a study performed by Horn et al. demonstrated

that CM-MSC aggravated OGD-induced cellular damage in hippocampal culture slices [76]. Similarly, Schreibe et al. observed neurotoxic effects of CM-MSC on neuronal cultures incubated with concentrations higher than 10% [75]. Since our pCN cultures were exposed to 100% CM, it cannot be excluded that this could have affected neuronal viability.

Additionally, the effect of BDNF, GDNF and IGF-II on neuronal survival was assessed to obtain information on which paracrine factor(s) could be responsible for (DPSC-mediated) neuroprotection Multiple studies have described the neuroprotective capacity of BDNF, GDNF and IGF-II *in vitro*. Van Kanegan et al. reported that addition of exogenous BDNF at a concentration of 200 ng/ml conferred neuroprotection to OGD-treated brain slices [77]. In accordance, pre-incubation of hippocampal neurons with 200 ng/ml BDNF reduced glutamate-mediated neurotoxicity [78]. Furthermore, it has been shown that GDNF treatment decreased 6-hydroxydopamine-induced toxicity in dopaminergic neurons [79]. Moreover, hippocampal culture slides incubated with IGF-II (2 µg/ml) demonstrated reduced OGD-induced neuronal damage [80]. In addition, 100 ng/ml IGF-II exerted neuroprotection to cortical neuronal cultures exposed to glucocorticoid-induced toxicity [81]. Despite of the known neuroprotective effects of BDNF, GDNF and IGF-II, we observed that addition of various concentrations of these neurotrophic factors did not improve neuronal survival after OGD.

In the present study, neuroprotection of ischaemic pCN could not be established by CM-DPSC or by neurotrophic factors. This might be due to the relative long exposure time of pCN cultures to OGD, which could induce irreversible damage in pCN. Most studies that employ the OGD survival assay culture neuronal cells on OGD conditions for approximately 90–120 min, while in our study, pCN were exposed to 3 h and 6 h OGD [56, 74, 75]. Moreover, Schreibe at al. and Liu et al. prepared CM-BM-MSC in standard neuronal culture medium (neurobasal medium), which is more favourable for the ischaemic neuronal cultures than α-MEM used in our study [74, 75]. α-MEM is a very nutrient poor medium compared to standard pCN culture medium, which can pose additional stress on pCN. Furthermore, our neuronal viability read-out might not be optimal. PI is a fluorescent dye which intercalates in DNA. Because of its impermeability for viable cells, PI specifically stains late apoptotic or necrotic cells. Considering that early apoptotic cells can be rescued in the early phases of ischaemia, PI staining does not provide information on these salvageable cells as only late apoptotic/necrotic cells are detected. Therefore, it would be more ideal to use early cell death marker stainings, such as caspase 3/7 or annexin V, as read-outs for neuronal death.

After cerebral ischaemia, endogenous repair mechanisms are not sufficiently activated. However, DPSC-based therapy represents a promising approach to stimulate these endogenous neuroregeneration mechanisms. Paracrine factors secreted by DPSC can presumably enhance the recruitment of NSC toward the stroke lesion, which is a critical first step in neuronal repair. Therefore in this study, the neuroregenerative capacity of DPSC were evaluated by assessing the effect of CM-DPSC, CM-HDF and CM-BM-MSC on NSC migration. We demonstrated that CM-DPSC possessed a significant higher migratory effect on NSC than CM-HDF and control medium. Furthermore, we showed that CM-DPSC seemed to stimulate NSC migration to a greater extent than CM-BM-MSC. Previous studies have demonstrated that DPSC transplanted in the hippocampus

of healthy mice were able to stimulate the proliferation and migration of NPC toward the graft site [58]. Furthermore, transplantation of DPSC in a rat model for ischaemic stroke enhanced the migration and differentiation of NPC in the peri-infarct area [61]. In line with our results, prior studies that explored the neuroregenerative effects of DPSC observed increased SH-SY5Y neuroblastoma progenitor cell migration *in vitro* in response to CM-DPSC compared to control medium [61, 82]. SH-SY5Y neuroblastoma cells are commonly used as an alternative for human NSC or progenitor cells with neuronal characteristics. However, data generated with this cell line must be carefully interpreted, since the SH-SY5Y neuroblastoma cells are derived from cancerous tissue and therefore possess other properties than NSC.

Migration of NSC toward the ischaemic lesion site has been described to be mediated via the SDF-1/CXCR-4 axis [47, 83]. NSC have been shown to express the CXCR-4 receptor, which is the cognate receptor for SDF-1. Moreover, NSC proliferation and transmigration was stimulated *in vitro* by SDF-1 exposure [47]. Since DPSC are known to secrete SDF-1 at concentrations of 0.015 pg/cell, the migratory effect of DPSC on NSC observed in this study could partially be mediated by SDF-1 present in CM-DPSC [57]. Furthermore, Arthur et al. compared the concentrations of SDF-1 in CM-DPSC with SDF-1 levels in CM of human foreskin fibroblasts [57]. They observed that CM-DPSC contained higher levels of SDF-1 than CM of human foreskin fibroblasts, which could explain the differential effect of CM-HDF and CM-DPSC on NSC migration in the present study. However, SDF-1 levels expressed by DPSC are similar to SDF-1 expression by BM-MSC [84]. Therefore, the greater migratory effect of DPSC in comparison to BM-MSC could be related to the higher levels of neurotrophic factors secreted by DPSC [55]. These paracrine factors, such as BDNF, NGF and NT-3 have been shown to play important roles in endogenous neurogenesis and might be responsible for DPSC-mediated NSC migration in addition to SDF-1 [85, 86].

Next, the migratory effect of multiple paracrine factors on NSC was assessed to get an indication on which paracrine factor(s) could be responsible for the observed DPSC-mediated NSC migration. In accordance with previous studies by Xue et al. and Imitola et al., we showed that SDF-1 exerted a great migratory effect on NSC *in vitro* [47, 83]. Additionally, we demonstrated that IGF-II promoted NSC migration compared to control. IGFs represent a highly conserved family of signalling peptides, which are crucial for stem cell proliferation and CNS development. Zackenfels et al. investigated the effect of IGFs on the development of chick sympathetic neurons. Their research group observed that insulin-like growth factor I (IGF-I) and IGF-II promoted neurite outgrowth in these neurons, which was a first indication of the neuroregenerative effects of IGF-II [87]. The neuroregenerative capacity of IGFs was further described by O'Kusky et al., who reported that IGF-II/IGF-I transgenic mice displayed increased postnatal synaptogenesis and neurogenesis compared to control mice [88]. Additionally, Ziegler et al. showed that IGF-II promoted the expansion of NSC *in vitro* [89, 90]. Moreover, silencing of IGF-II with short hairpin RNA (shRNA) resulted in reduced proliferation of adult hippocampal NSC *in vitro* and *in vivo* [91]. These findings indicate crucial roles of IGF-II in adult neurogenesis. However, no data could be found on the effect of IGF-II on NSC migration, which suggest that our study is the first that demonstrates the migratory effect of IGF-II on NSC.

Due to the beneficial effects on NSC migration, upregulation of IGF-II via lentiviral transduction represent an interesting approach to boost the neuroregenerative effects of DPSC in future experiments. Therefore, it was investigated whether addition of IGF-II to CM-DPSC could enhance its migratory effect on NSC. Nevertheless, no additional effect of IGF-II could be observed. Our growth factor array results demonstrated that IGFBP-6 is highly secreted by DPSC. IGFBP-6 is one of the six insulin-like growth factor binding proteins which binds and regulates the availability of IGF-I and –II. However, IGFBP-6 preferentially binds to IGF-II, since it possesses a 50 fold higher affinity for IGF-II than IGF-I [92, 93]. Furthermore, it is known that IGFBP-6 is a relative specific inhibitor of IGF-II mediated actions [92-94]. Based on its inhibitory effect, IGFBP-6 present in CM-DPSC could potentially bind to the added exogenous IGF-II and thereby neutralizing the migratory effect of IGF-II. In future experiments, the high expression of IGFBP-6 by DPSC has to be taken into account when overexpressing IGF-II in DPSC. For example, an IGF-II variant with lower IGFBP-6 affinity could be designed and incorporated in the lentiviral vector.

The next phase in this study is to decipher the responsible paracrine factors for DPSC-mediated NSC migration. This can be assessed by blocking the key paracrine factors (IGF-II and SDF-1) in CM-DPSC using neutralizing antibodies or by blocking their cognate receptors on NSC. Activation of the IGF receptor type 1 (IGF1R) has been described to play crucial roles in developmental and adult neurogenesis [95]. Bracko et al. reported that IGF-II stimulated hippocampal NSC proliferation via IGF1R-mediated AKT signalling [91]. Moreover, activation of IGF1R has been shown to influence the activation status of focal adhesion components, which correlated with lamellipodia motility in SH-SY5Y human neuroblastoma cells [95, 96]. These findings indicate the possible involvement of IGF1R and its downstream signalling cascades in IGF-II mediated NSC migration, which could further be investigated in the present study. In addition to IGF-II, IGF-I is an important ligand of the IGF1R receptor and therefore the contribution of IGF-I in NSC migration could be characterized. Furthermore, the role of IGFBP-6 in DPSC mediated NSC migration could be evaluated. Expression of IGFBP-6 in DPSC could be transiently silenced using shRNA. Subsequently, the migratory effect of IGFBP-6 deficient CM-DPSC could be compared to control CM-DPSC, to obtain information on the involvement of IGF-II in DPSC-mediated NSC migration.

To further examine the neuroprotective capacity of DPSC, other neurotoxicity assays in addition to the OGD survival assay could be employed. Glutamate excitotoxicity represents a very interesting assay for neuroprotection studies, since this process is a crucial part of the ischaemic cascade. However, optimization of the neurotoxic glutamate concentration and the glutamate exposure time has to be performed in order to use this assay for neuroprotection studies. In addition, further characterization of the neuroregenerative effect of DPSC could include investigation of NSC proliferation and differentiation in response to CM-DPSC. Moreover, the ability of CM-DPSC to promote neurite outgrowth and synaptogenesis in pCN cultures could be explored. In the above-mentioned experiments, key paracrine factors should be included to screen for their neuroprotective and -regenerative effects. The ultimate goal is to upregulate the most potent neuroprotective/regenerative paracrine factor in DPSC and to transplant these neurotrophic enhanced DPSC into the transient middle cerebral artery occlusion mouse model for ischaemic stroke.

5 Conclusion

Worldwide, ischaemic stroke is ranked as the second leading cause of death and is a major cause of permanent disability in patients. Despite the advances made in stroke healthcare, the number of people suffering from stroke is still rising. The aging population can be held responsible for the increase in stroke prevalence. Given that the number of individuals over the age of 65 will double by 2030, the amount of disabled patients following stroke will continue to rise. Since the current therapies are unable to sufficiently improve functional outcome following stroke, there is an increasing need for more effective therapies that promote functional recovery. Cell-based therapy is considered as a promising treatment strategy that aims to reduce neuronal damage and stimulate host repair. Because of their neurogenic properties, DPSC represent ideal candidates for this purpose. Therefore, the goal of this study was to characterize the neuroprotective and neuroregenerative effects of DPSC *in vitro*.

Protecting ischaemic neuronal cells from apoptosis by providing neurotrophic support could be a possible mechanism of action of DPSC-based therapy in stroke. In order to recreate the ischaemic conditions *in vitro*, an OGD neuronal survival assay was performed. Firstly, the surface coating for pCN in the OGD assay was optimized. We demonstrated that pCN cultured on 100 µg/ml PLO-coating display the highest cellular viability after OGD and characteristics of a mature neuronal network. In the next phase, the neuroprotective capacity of DPSC was evaluated by assessing the effect of CM-DPSC exposure on pCN survival following OGD. However in the present study, CM-DPSC is not able to improve neuronal survival. This might be due to the long OGD exposure time employed in our study which could induce irreversible damage in pCN. Alternatively, other assays such as the glutamate excitotoxicity assay could be explored for future neuroprotection studies.

Another possible mechanism of action of DPSC-based therapy is the stimulation of endogenous repair mechanisms. The attraction of NSC toward the lesion site is a crucial first step in endogenous neuroregeneration following stroke. Therefore, the neuroregenerative effects of DPSC were assessed by investigating NSC migration in response to CM-DPSC. Here, we showed that CM-DPSC exerts a significant higher migratory effect on NSC than CM-HDF and control medium. Furthermore, CM-DPSC seems to promote NSC migration to a greater extent than CM-BM-MSC. Additionally, the neuroregenerative capacity of key paracrine factors were evaluated. We demonstrated that IGF-II and SDF-1 significantly enhance NSC migration compared to control. In future experiments, it could be investigated whether these two paracrine factors are responsible for DPSC-mediated NSC migration by neutralizing these factors in CM-DPSC.

In conclusion, the capacity of DPSC to exert neuroprotective effects *in vitro* could not be demonstrated yet. However, a first indication of the neuroregenerative capacity of DPSC *in vitro* was established. More elaborate research on the *in vitro* neurorestorative effects of DPSC has to be performed to gain more insight in the paracrine-mediated beneficial mechanisms of DPSC in stroke. This will grant us crucial information on the therapeutic potential of DPSC in ischaemic stroke.

6 References

1. Mukherjee, D. and C.G. Patil, Epidemiology and the global burden of stroke. World Neurosurg, 2011. **76**(6 Suppl): p. S85-90.
2. Krishnamurthi, R.V., et al., Global and regional burden of first-ever ischaemic and haemorrhagic stroke during 1990-2010: findings from the Global Burden of Disease Study 2010. Lancet Glob Health, 2013. **1**(5): p. e259-81.
3. Di Carlo, A., Human and economic burden of stroke. Age Ageing, 2009. **38**(1): p. 4-5.
4. Durukan, A. and T. Tatlisumak, Acute ischemic stroke: overview of major experimental rodent models, pathophysiology, and therapy of focal cerebral ischemia. Pharmacol Biochem Behav, 2007. **87**(1): p. 179-97.
5. MB, M., Ischemic Stroke : Pathophysiology and Principles of Localization. Neurology Board review manual, 2009: p. p. 1-16.
6. Molina, C.A., Reperfusion therapies for acute ischemic stroke: current pharmacological and mechanical approaches. Stroke, 2011. **42**(1 Suppl): p. S16-9.
7. Brouns, R. and P.P. De Deyn, The complexity of neurobiological processes in acute ischemic stroke. Clin Neurol Neurosurg, 2009. **111**(6): p. 483-95.
8. Dirnagl, U., C. Iadecola, and M.A. Moskowitz, Pathobiology of ischaemic stroke: an integrated view. Trends Neurosci, 1999. **22**(9): p. 391-7.
9. Doyle, K.P., R.P. Simon, and M.P. Stenzel-Poore, Mechanisms of ischemic brain damage. Neuropharmacology, 2008. **55**(3): p. 310-8.
10. Gervois, P., et al., Stem Cell-Based Therapies for Ischemic Stroke: Preclinical Results and the Potential of Imaging-Assisted Evaluation of Donor Cell Fate and Mechanisms of Brain Regeneration. Med Res Rev, 2016.
11. Schmidt, A., J. Minnerup, and C. Kleinschnitz, Emerging neuroprotective drugs for the treatment of acute ischaemic stroke. Expert Opin Emerg Drugs, 2013. **18**(2): p. 109-20.
12. Sutherland, B.A., et al., Neuroprotection for ischaemic stroke: translation from the bench to the bedside. Int J Stroke, 2012. **7**(5): p. 407-18.
13. Del Zoppo, G.J., et al., Expansion of the time window for treatment of acute ischemic stroke with intravenous tissue plasminogen activator: a science advisory from the American Heart Association/American Stroke Association. Stroke, 2009. **40**(8): p. 2945-8.
14. Pan, J., et al., Reperfusion injury following cerebral ischemia: pathophysiology, MR imaging, and potential therapies. Neuroradiology, 2007. **49**(2): p. 93-102.
15. Lindvall, O. and Z. Kokaia, Stem cell research in stroke: how far from the clinic? Stroke, 2011. **42**(8): p. 2369-75.
16. Martens, W., et al., Dental stem cells and their promising role in neural regeneration: an update. Clin Oral Investig, 2013. **17**(9): p. 1969-83.
17. Burns, T.C., C.M. Verfaillie, and W.C. Low, Stem cells for ischemic brain injury: a critical review. J Comp Neurol, 2009. **515**(1): p. 125-44.
18. Lakshmipathy, U. and C. Verfaillie, Stem cell plasticity. Blood Rev, 2005. **19**(1): p. 29-38.

19. Chamberlain, G., et al., Concise review: mesenchymal stem cells: their phenotype, differentiation capacity, immunological features, and potential for homing. Stem Cells, 2007. **25**(11): p. 2739-49.
20. Hilkens, P., et al., Cryopreservation and Banking of Dental Stem Cells. Adv Exp Med Biol, 2016. **951**: p. 199-235.
21. Phinney, D.G. and D.J. Prockop, Concise review: mesenchymal stem/multipotent stromal cells: the state of transdifferentiation and modes of tissue repair--current views. Stem Cells, 2007. **25**(11): p. 2896-902.
22. Gronthos, S., et al., Postnatal human dental pulp stem cells (DPSCs) in vitro and in vivo. Proc Natl Acad Sci U S A, 2000. **97**(25): p. 13625-30.
23. Janebodin, K., et al., Isolation and characterization of neural crest-derived stem cells from dental pulp of neonatal mice. PLoS One, 2011. **6**(11): p. e27526.
24. Gronthos, S., et al., Stem cell properties of human dental pulp stem cells. J Dent Res, 2002. **81**(8): p. 531-5.
25. Jo, Y.Y., et al., Isolation and characterization of postnatal stem cells from human dental tissues. Tissue Eng, 2007. **13**(4): p. 767-73.
26. Arthur, A., et al., Adult human dental pulp stem cells differentiate toward functionally active neurons under appropriate environmental cues. Stem Cells, 2008. **26**(7): p. 1787-95.
27. Gervois, P., et al., Neurogenic maturation of human dental pulp stem cells following neurosphere generation induces morphological and electrophysiological characteristics of functional neurons. Stem Cells Dev, 2015. **24**(3): p. 296-311.
28. Hilkens, P., et al., Effect of isolation methodology on stem cell properties and multilineage differentiation potential of human dental pulp stem cells. Cell Tissue Res, 2013. **353**(1): p. 65-78.
29. Pierdomenico, L., et al., Multipotent mesenchymal stem cells with immunosuppressive activity can be easily isolated from dental pulp. Transplantation, 2005. **80**(6): p. 836-42.
30. Perry, B.C., et al., Collection, cryopreservation, and characterization of human dental pulp-derived mesenchymal stem cells for banking and clinical use. Tissue Eng Part C Methods, 2008. **14**(2): p. 149-56.
31. Graziano, A., et al., Dental pulp stem cells: a promising tool for bone regeneration. Stem Cell Rev, 2008. **4**(1): p. 21-6.
32. Bronckaers, A., et al., Angiogenic properties of human dental pulp stem cells. PLoS One, 2013. **8**(8): p. e71104.
33. Gandia, C., et al., Human dental pulp stem cells improve left ventricular function, induce angiogenesis, and reduce infarct size in rats with acute myocardial infarction. Stem Cells, 2008. **26**(3): p. 638-45.
34. Martens, W., et al., Expression pattern of basal markers in human dental pulp stem cells and tissue. Cells Tissues Organs, 2012. **196**(6): p. 490-500.
35. Nosrat, I.V., et al., Dental pulp cells provide neurotrophic support for dopaminergic neurons and differentiate into neurons in vitro; implications for tissue engineering and repair in the nervous system. Eur J Neurosci, 2004. **19**(9): p. 2388-98.

36. Nosrat, I.V., et al., Dental pulp cells produce neurotrophic factors, interact with trigeminal neurons in vitro, and rescue motoneurons after spinal cord injury. Dev Biol, 2001. **238**(1): p. 120-32.
37. Gutierrez-Fernandez, M., et al., Trophic factors and cell therapy to stimulate brain repair after ischaemic stroke. J Cell Mol Med, 2012. **16**(10): p. 2280-90.
38. Lee, J.S., et al., A long-term follow-up study of intravenous autologous mesenchymal stem cell transplantation in patients with ischemic stroke. Stem Cells, 2010. **28**(6): p. 1099-106.
39. Mine, Y., et al., Grafted human neural stem cells enhance several steps of endogenous neurogenesis and improve behavioral recovery after middle cerebral artery occlusion in rats. Neurobiol Dis, 2013. **52**: p. 191-203.
40. Banerjee, S., et al., The potential benefit of stem cell therapy after stroke: an update. Vasc Health Risk Manag, 2012. **8**: p. 569-80.
41. Li, G., et al., Bone marrow mesenchymal stem cell therapy in ischemic stroke: mechanisms of action and treatment optimization strategies. Neural Regen Res, 2016. **11**(6): p. 1015-24.
42. Krabbe, C., J. Zimmer, and M. Meyer, Neural transdifferentiation of mesenchymal stem cells--a critical review. APMIS, 2005. **113**(11-12): p. 831-44.
43. Anghileri, E., et al., Neuronal differentiation potential of human adipose-derived mesenchymal stem cells. Stem Cells Dev, 2008. **17**(5): p. 909-16.
44. Kiraly, M., et al., Integration of neuronally predifferentiated human dental pulp stem cells into rat brain in vivo. Neurochem Int, 2011. **59**(3): p. 371-81.
45. Leong, W.K., et al., Human adult dental pulp stem cells enhance poststroke functional recovery through non-neural replacement mechanisms. Stem Cells Transl Med, 2012. **1**(3): p. 177-87.
46. Wakabayashi, K., et al., Transplantation of human mesenchymal stem cells promotes functional improvement and increased expression of neurotrophic factors in a rat focal cerebral ischemia model. J Neurosci Res, 2010. **88**(5): p. 1017-25.
47. Imitola, J., et al., Directed migration of neural stem cells to sites of CNS injury by the stromal cell-derived factor 1alpha/CXC chemokine receptor 4 pathway. Proc Natl Acad Sci U S A, 2004. **101**(52): p. 18117-22.
48. Hill, W.D., et al., SDF-1 (CXCL12) is upregulated in the ischemic penumbra following stroke: association with bone marrow cell homing to injury. J Neuropathol Exp Neurol, 2004. **63**(1): p. 84-96.
49. Bao, X., et al., Transplantation of human bone marrow-derived mesenchymal stem cells promotes behavioral recovery and endogenous neurogenesis after cerebral ischemia in rats. Brain Res, 2011. **1367**: p. 103-13.
50. Yoo, S.W., et al., Mesenchymal stem cells promote proliferation of endogenous neural stem cells and survival of newborn cells in a rat stroke model. Exp Mol Med, 2008. **40**(4): p. 387-97.
51. Chen, J., et al., Intravenous administration of human bone marrow stromal cells induces angiogenesis in the ischemic boundary zone after stroke in rats. Circ Res, 2003. **92**(6): p. 692-9.

52. Uccelli, A., L. Moretta, and V. Pistoia, Mesenchymal stem cells in health and disease. Nat Rev Immunol, 2008. **8**(9): p. 726-36.
53. Boehm-Sturm, P., et al., A multi-modality platform to image stem cell graft survival in the naive and stroke-damaged mouse brain. Biomaterials, 2014. **35**(7): p. 2218-26.
54. Aswendt, M., J. Adamczak, and A. Tennstaedt, A review of novel optical imaging strategies of the stroke pathology and stem cell therapy in stroke. Front Cell Neurosci, 2014. **8**: p. 226.
55. Mead, B., et al., Paracrine-mediated neuroprotection and neuritogenesis of axotomised retinal ganglion cells by human dental pulp stem cells: comparison with human bone marrow and adipose-derived mesenchymal stem cells. PLoS One, 2014. **9**(10): p. e109305.
56. Song, M., et al., Comparison of the effects of human dental pulp stem cells and human bone marrow-derived mesenchymal stem cells on ischemic human astrocytes in vitro. J Neurosci Res, 2015. **93**(6): p. 973-83.
57. Arthur, A., et al., Implanted adult human dental pulp stem cells induce endogenous axon guidance. Stem Cells, 2009. **27**(9): p. 2229-37.
58. Huang, A.H., et al., Putative dental pulp-derived stem/stromal cells promote proliferation and differentiation of endogenous neural cells in the hippocampus of mice. Stem Cells, 2008. **26**(10): p. 2654-63.
59. Apel, C., et al., The neuroprotective effect of dental pulp cells in models of Alzheimer's and Parkinson's disease. J Neural Transm (Vienna), 2009. **116**(1): p. 71-8.
60. Fang, C.Z., et al., Intraventricular injection of human dental pulp stem cells improves hypoxic-ischemic brain damage in neonatal rats. PLoS One, 2013. **8**(6): p. e66748.
61. Sugiyama, M., et al., Dental pulp-derived CD31(-)/CD146(-) side population stem/progenitor cells enhance recovery of focal cerebral ischemia in rats. Tissue Eng Part A, 2011. **17**(9-10): p. 1303-11.
62. Zheng, Y.H., et al., Multilineage differentiation of human bone marrow mesenchymal stem cells in vitro and in vivo. Exp Ther Med, 2013. **5**(6): p. 1576-1580.
63. Struys, T., et al., Ultrastructural and immunocytochemical analysis of multilineage differentiated human dental pulp- and umbilical cord-derived mesenchymal stem cells. Cells Tissues Organs, 2011. **193**(6): p. 366-78.
64. Nuti, N., et al., Multipotent Differentiation of Human Dental Pulp Stem Cells: a Literature Review. Stem Cell Rev, 2016. **12**(5): p. 511-523.
65. Crigler, L., et al., Isolation of a mesenchymal cell population from murine dermis that contains progenitors of multiple cell lineages. FASEB J, 2007. **21**(9): p. 2050-63.
66. Toma, J.G., et al., Isolation of multipotent adult stem cells from the dermis of mammalian skin. Nat Cell Biol, 2001. **3**(9): p. 778-84.
67. Lorenz, K., et al., Multilineage differentiation potential of human dermal skin-derived fibroblasts. Exp Dermatol, 2008. **17**(11): p. 925-32.
68. Huang, H.I., et al., Multilineage differentiation potential of fibroblast-like stromal cells derived from human skin. Tissue Eng Part A, 2010. **16**(5): p. 1491-501.
69. Scott, M.A., et al., Current methods of adipogenic differentiation of mesenchymal stem cells. Stem Cells Dev, 2011. **20**(10): p. 1793-804.

70. Mead, B., et al., Intravitreally transplanted dental pulp stem cells promote neuroprotection and axon regeneration of retinal ganglion cells after optic nerve injury. Invest Ophthalmol Vis Sci, 2013. **54**(12): p. 7544-56.
71. Ahlemeyer, B., et al., Staurosporine-induced apoptosis in cultured chick embryonic neurons is reduced by polyethylenimine of low molecular weight used as a coating substrate. Neurosci Res, 2000. **37**(4): p. 245-53.
72. Chen, W.H., et al., Probing relevant molecules in modulating the neurite outgrowth of hippocampal neurons on substrates of different stiffness. PLoS One, 2013. **8**(12): p. e83394.
73. Ahlemeyer, B. and E. Baumgart-Vogt, Optimized protocols for the simultaneous preparation of primary neuronal cultures of the neocortex, hippocampus and cerebellum from individual newborn (P0.5) C57Bl/6J mice. J Neurosci Methods, 2005. **149**(2): p. 110-20.
74. Liu, Y., et al., Effects of bone marrow-derived mesenchymal stem cells on the axonal outgrowth through activation of PI3K/AKT signaling in primary cortical neurons followed oxygen-glucose deprivation injury. PLoS One, 2013. **8**(11): p. e78514.
75. Scheibe, F., et al., Mesenchymal stromal cells rescue cortical neurons from apoptotic cell death in an in vitro model of cerebral ischemia. Cell Mol Neurobiol, 2012. **32**(4): p. 567-76.
76. Horn, A.P., et al., Conditioned medium from mesenchymal stem cells induces cell death in organotypic cultures of rat hippocampus and aggravates lesion in a model of oxygen and glucose deprivation. Neurosci Res, 2009. **63**(1): p. 35-41.
77. Van Kanegan, M.J., et al., BDNF mediates neuroprotection against oxygen-glucose deprivation by the cardiac glycoside oleandrin. J Neurosci, 2014. **34**(3): p. 963-8.
78. Almeida, R.D., et al., Neuroprotection by BDNF against glutamate-induced apoptotic cell death is mediated by ERK and PI3-kinase pathways. Cell Death Differ, 2005. **12**(10): p. 1329-43.
79. Eggert, K., et al., Glial cell line-derived neurotrophic factor protects dopaminergic neurons from 6-hydroxydopamine toxicity in vitro. Neurosci Lett, 1999. **269**(3): p. 178-82.
80. Mackay, K.B., et al., Neuroprotective effects of insulin-like growth factor-binding protein ligand inhibitors in vitro and in vivo. J Cereb Blood Flow Metab, 2003. **23**(10): p. 1160-7.
81. Martin-Montanez, E., et al., Involvement of IGF-II receptors in the antioxidant and neuroprotective effects of IGF-II on adult cortical neuronal cultures. Biochim Biophys Acta, 2014. **1842**(7): p. 1041-51.
82. Gervois, P., et al., Paracrine Maturation and Migration of SH-SY5Y Cells by Dental Pulp Stem Cells. J Dent Res, 2017. **96**(6): p. 654-662.
83. Xue, L., et al., The effect of stromal cell-derived factor 1 in the migration of neural stem cells. Cell Biochem Biophys, 2014. **70**(3): p. 1609-16.
84. Kortesidis, A., et al., Stromal-derived factor-1 promotes the growth, survival, and development of human bone marrow stromal stem cells. Blood, 2005. **105**(10): p. 3793-801.
85. Oliveira, S.L., et al., Functions of neurotrophins and growth factors in neurogenesis and brain repair. Cytometry A, 2013. **83**(1): p. 76-89.
86. Lee, E. and H. Son, Adult hippocampal neurogenesis and related neurotrophic factors. BMB Rep, 2009. **42**(5): p. 239-44.

87. Zackenfels, K., R.W. Oppenheim, and H. Rohrer, Evidence for an important role of IGF-I and IGF-II for the early development of chick sympathetic neurons. Neuron, 1995. **14**(4): p. 731-41.
88. O'Kusky, J.R., P. Ye, and A.J. D'Ercole, Insulin-like growth factor-I promotes neurogenesis and synaptogenesis in the hippocampal dentate gyrus during postnatal development. J Neurosci, 2000. **20**(22): p. 8435-42.
89. Ziegler, A.N., et al., Insulin-like growth factor-II (IGF-II) and IGF-II analogs with enhanced insulin receptor-a binding affinity promote neural stem cell expansion. J Biol Chem, 2014. **289**(8): p. 4626-33.
90. Ziegler, A.N., et al., IGF-II promotes stemness of neural restricted precursors. Stem Cells, 2012. **30**(6): p. 1265-76.
91. Bracko, O., et al., Gene expression profiling of neural stem cells and their neuronal progeny reveals IGF2 as a regulator of adult hippocampal neurogenesis. J Neurosci, 2012. **32**(10): p. 3376-87.
92. Baxter, R.C., Insulin-like growth factor (IGF)-binding proteins: interactions with IGFs and intrinsic bioactivities. Am J Physiol Endocrinol Metab, 2000. **278**(6): p. E967-76.
93. Bach, L.A., IGFBP-6 five years on; not so 'forgotten'? Growth Horm IGF Res, 2005. **15**(3): p. 185-92.
94. Raykha, C., et al., IGF-II and IGFBP-6 regulate cellular contractility and proliferation in Dupuytren's disease. Biochim Biophys Acta, 2013. **1832**(10): p. 1511-9.
95. Annenkov, A., The insulin-like growth factor (IGF) receptor type 1 (IGF1R) as an essential component of the signalling network regulating neurogenesis. Mol Neurobiol, 2009. **40**(3): p. 195-215.
96. Leventhal, P.S., et al., Tyrosine phosphorylation of paxillin and focal adhesion kinase during insulin-like growth factor-I-stimulated lamellipodial advance. J Biol Chem, 1997. **272**(8): p. 5214-8.

Auteursrechtelijke overeenkomst

Ik/wij verlenen het wereldwijde auteursrecht voor de ingediende eindverhandeling:
Dental pulp stem cell therapy in ischaemic stroke: exploring the neuroprotective and -regenerative effects in vitro

Richting: **master in de biomedische wetenschappen-klinische moleculaire wetenschappen**
Jaar: **2017**

in alle mogelijke mediaformaten, - bestaande en in de toekomst te ontwikkelen - , aan de Universiteit Hasselt.

Niet tegenstaand deze toekenning van het auteursrecht aan de Universiteit Hasselt behoud ik als auteur het recht om de eindverhandeling, - in zijn geheel of gedeeltelijk -, vrij te reproduceren, (her)publiceren of distribueren zonder de toelating te moeten verkrijgen van de Universiteit Hasselt.

Ik bevestig dat de eindverhandeling mijn origineel werk is, en dat ik het recht heb om de rechten te verlenen die in deze overeenkomst worden beschreven. Ik verklaar tevens dat de eindverhandeling, naar mijn weten, het auteursrecht van anderen niet overtreedt.

Ik verklaar tevens dat ik voor het materiaal in de eindverhandeling dat beschermd wordt door het auteursrecht, de nodige toelatingen heb verkregen zodat ik deze ook aan de Universiteit Hasselt kan overdragen en dat dit duidelijk in de tekst en inhoud van de eindverhandeling werd genotificeerd.

Universiteit Hasselt zal mij als auteur(s) van de eindverhandeling identificeren en zal geen wijzigingen aanbrengen aan de eindverhandeling, uitgezonderd deze toegelaten door deze overeenkomst.

Voor akkoord,

Kemps, Hannelore

Datum: **8/06/2017**